Chemistry–A European Journal

Supporting Information

Elucidating Atropisomerism in Nonplanar Porphyrins with Tunable Supramolecular Complexes

Karolis Norvaiša,[a] John E. O'Brien,[a] Dáire J. Gibbons,[a] and Mathias O. Senge*[a, b]

Table of Contents

SUPPORTING INFORMATION

Experimental Procedures

General Methods

NMR spectra were recorded on a Bruker Advance III 400 MHz, a Bruker Advance HD 400 and an Agilent 400 spectrometer for ^{1}H (400.13 MHz) and ^{13}C (100.61 MHz) NMR spectra. A Bruker Ultrashield 600 spectrometer was employed for ^{1}H (600.13 MHz), ^{13}C (150.90 MHz) and ^{15}N NMR (61 MHz) spectra. All NMR experiments were performed at 25 ºC. Resonances δ are given in ppm units and referenced to the deuterium signal in the NMR solvents, acetonitrile-d_3 (δ_H = 1.94 ppm, δ_C = 1.32, 118.26 ppm). Signal multiplicities are abbreviated as follows: singlet = s, doublet = d, triplet = t, dq = doublet of quartets, multiplet = m.

Single crystal X-ray crystallography: Diffraction data for all compounds were collected on a Bruker APEX 2 DUO CCD diffractometer using graphite-monochromated Mo-K_α (λ = 0.71073 Å) and Incoatec IμS Cu-K_α (λ = 1.54178 Å) radiation. Crystals were mounted on a MiTeGen MicroMount and collected at 100(2) K using an Oxford Cryosystems Cobra low-temperature device. Data were collected using omega and phi scans and were corrected for Lorentz and polarization effects using the APEX software suite.[S1] Data were corrected for absorption effects using the multi-scan method (SADABS).[S2]

Shelnutt's NSD (normal structural decomposition) method was used to delineate, quantify and illustrate the various distortions modes present in the tetrapyrrole macrocycles.[S3] NSD calculations were performed with the NSD GUI version of the program.[S4]

Crystals were grown following the protocol developed by Hope, e.g. oversaturated porphyrin/ DMSO solution, slow evaporation in acetonitrile or slow liquid-liquid diffusion of $CHCl_3$ and MeOH.[S5] Using Olex2, the structure was solved with the XT structure solution program, using the intrinsic phasing solution method and refined against $|F^2|$ with XL using least-squares minimization.[S6] If electron density was not sufficient, the C and N bound H atoms were placed in their expected calculated positions and refined using a riding model: N–H = 0.88 Å, C–H = 0.95–0.98 Å, with U_{iso} (H) = 1.5U_{eq} (C) for methyl H atoms and 1.2U_{eq} (C, N). Details of data refinements can be found in Table S1-S2. All images were prepared using Olex2.[S6a]

SUPPORTING INFORMATION

Synthesis and Characterization of Compounds

*Synthesis and Characterization of α,β,α,β-***P1-BSA**

α,β,α,β-5,10,15,20-Tetrakis(2-aminiumphenyl)-2,3,7,8,12,13,17,18-octaethylporphyrin hexa-benzenesulfonic acid salt (*α,β,α,β*-P1-BSA). In a sample tube benzene sulfonic acid (0.82 mg; 0.25 mmol; 50 eq.) was dissolved in 1 mL of acetonitrile-*d*$_3$. Isomerically pure [α,β,α,β-5,10,15,20-tetrakis(2-aminophenyl)-2,3,7,8,12,13,17,18-octaethylporphyrinato]nickel(II) (5 mg; 0.005 mmol; 1 eq.) was added in one batch and stirred for 16 hours. The completion of demetalation followed by complex formation was identified by a distinct color change (maroon to green) of the solution. ^{1}H NMR (600 MHz, acetonitrile-*d*$_3$) δ = 8.92 (d, *J* = 7.5 Hz, 4H, Ar-*H*), 8.11 (t, *J* = 7.7 Hz, 4H, Ar-*H*), 8.02 (d, *J* = 8.1 Hz, 4H, Ar-*H*), 7.99 (t, *J* = 7.6 Hz, 4H, Ar-*H*), 2.63 (dq, *J* = 14.9, 7.6 Hz, 4H, C*H*$_2$ (a))2.38 (dq, *J* = 15.1, 7.5 Hz, 4H, C*H*$_2$ (b)), 2.06 (dq, *J* = 15.1, 7.7 Hz, 4H, C*H*$_2$ (b)), 1.86 (dq, *J* = 15.4, 7.7 Hz, 4H, C*H*$_2$ (a)), 0.62 (t, *J* = 7.6 Hz, 12H, C*H*$_3$ (b)), 0.05 (t, *J* = 7.5 Hz, 12H, C*H*$_3$ (a)), -1.42 (s, 4H) ppm.; ^{13}C NMR (151 MHz, acetonitrile-*d*$_3$) δ = 145.01 (α-pyrrole (b)), 144 (β-pyrrole (b)), 143.82 (β-pyrrole (a)), 143.63 (α-pyrrole (a)), 140.12 (Ar), 134.41 (Ar), 132.86 (Ar), 132.11 (Ar), 130.91 (Ar), 126.02 (Ar), 113.12 (meso-), 20.62 (CH_2 (b)), 19.81 (CH_2 (a)), 15.56 (CH_3 (b)), 15.28 (CH_3 (a)) ppm.; ^{15}N NMR (61 MHz, acetonitrile-*d*$_3$) δ 126.46 (N-H) ppm.

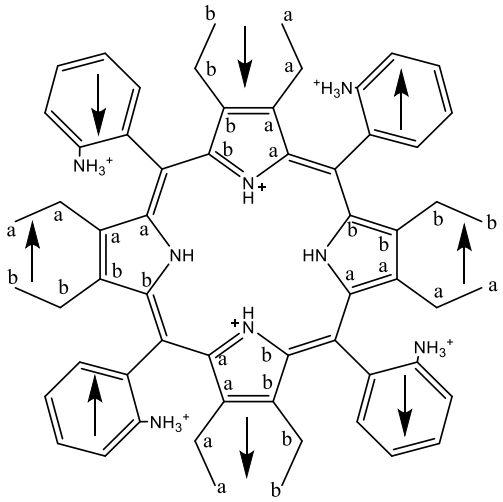

Figure S1. Structure of *α,β,α,β*-**P1-BSA** highlighting the positions used in the NMR characterizations.

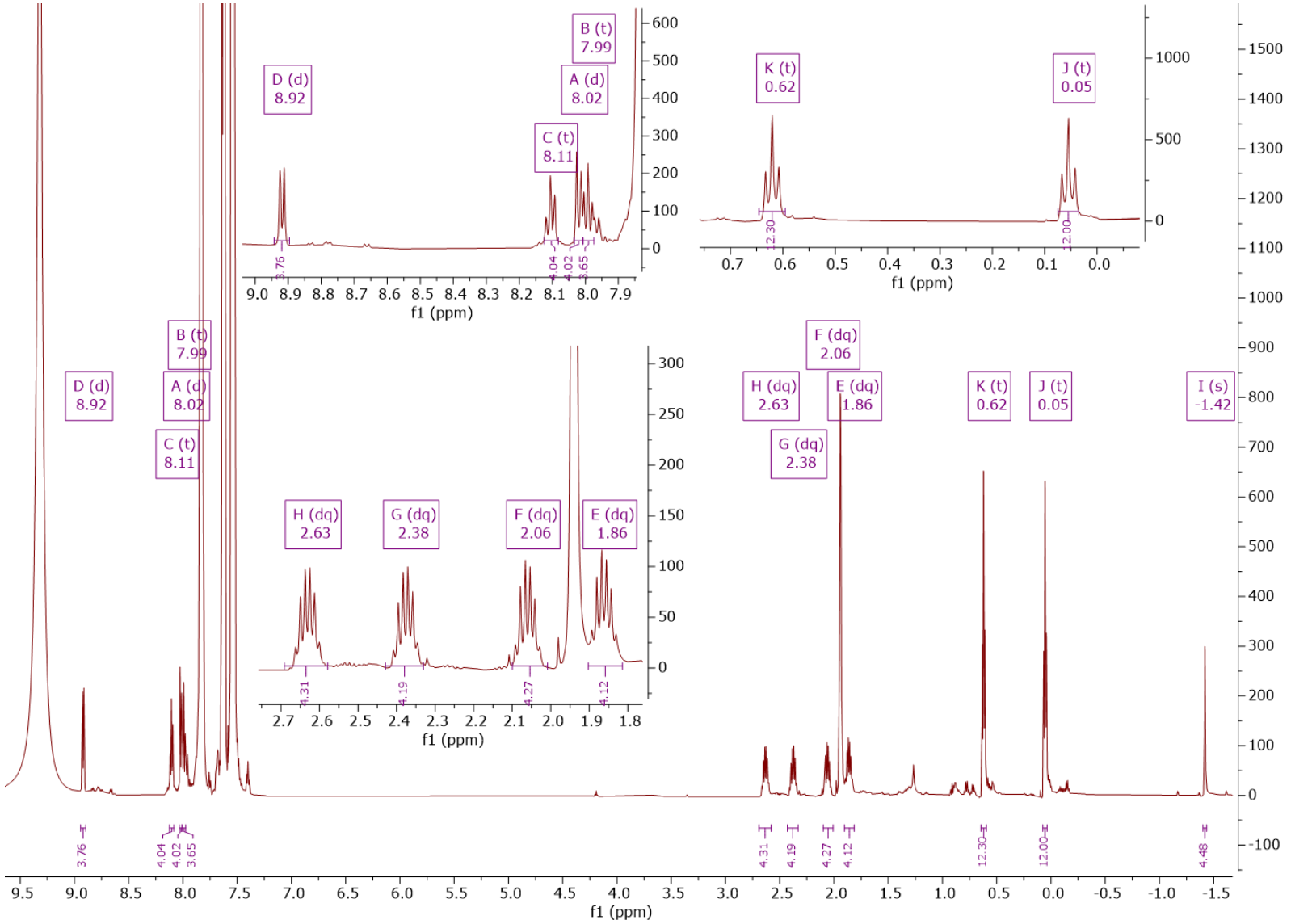

Figure S2. ^{1}H NMR spectrum of *α,β,α,β*-**P1-BSA** with expansion of areas of interest (600 MHz, acetonitrile-d_3, 25 °C).

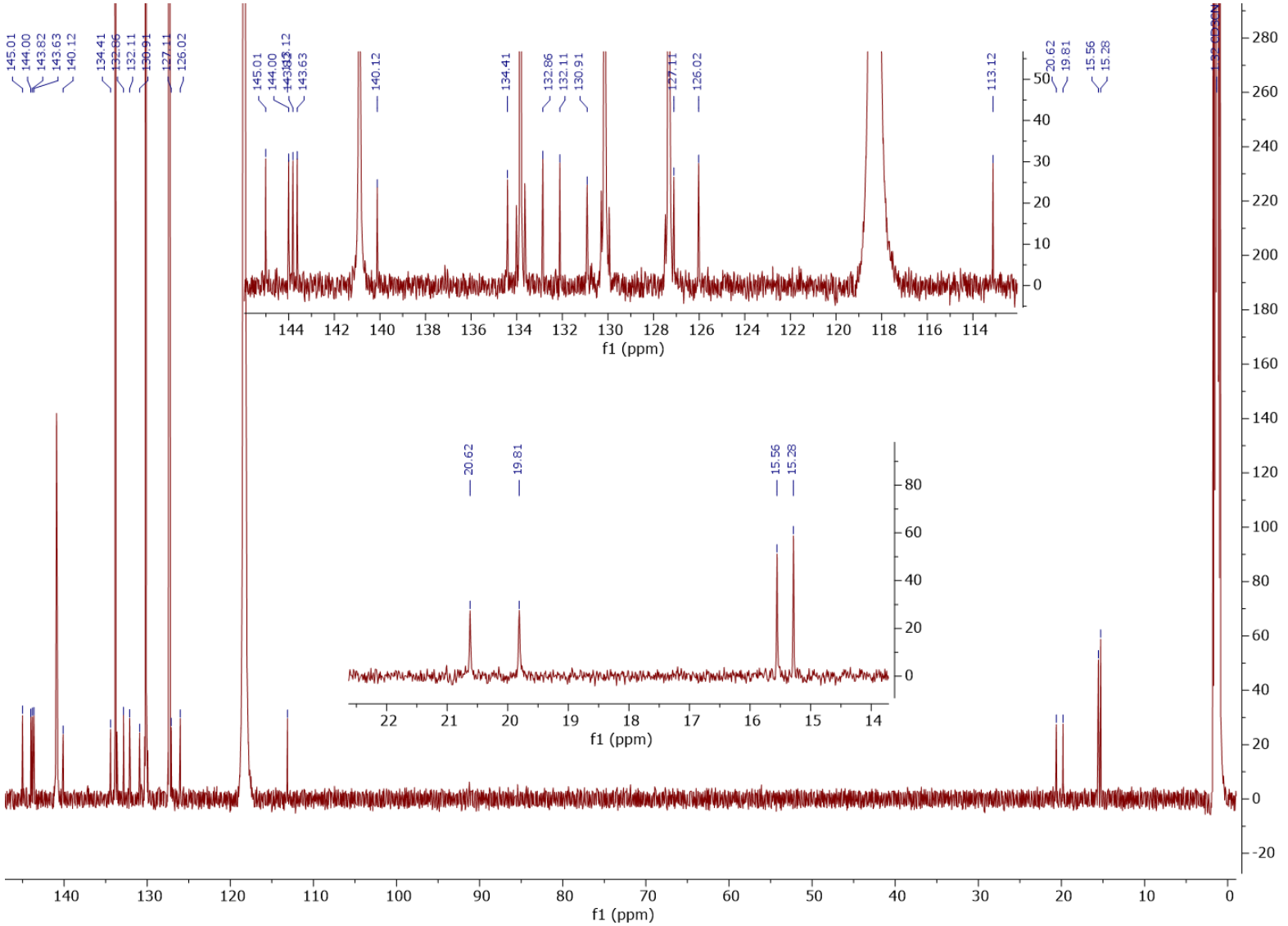

Figure S3. ^{13}C NMR spectrum of *α,β,α,β*-**P1-BSA** with expansion of areas of interest (151 MHz, acetonitrile-d_3, 25 °C).

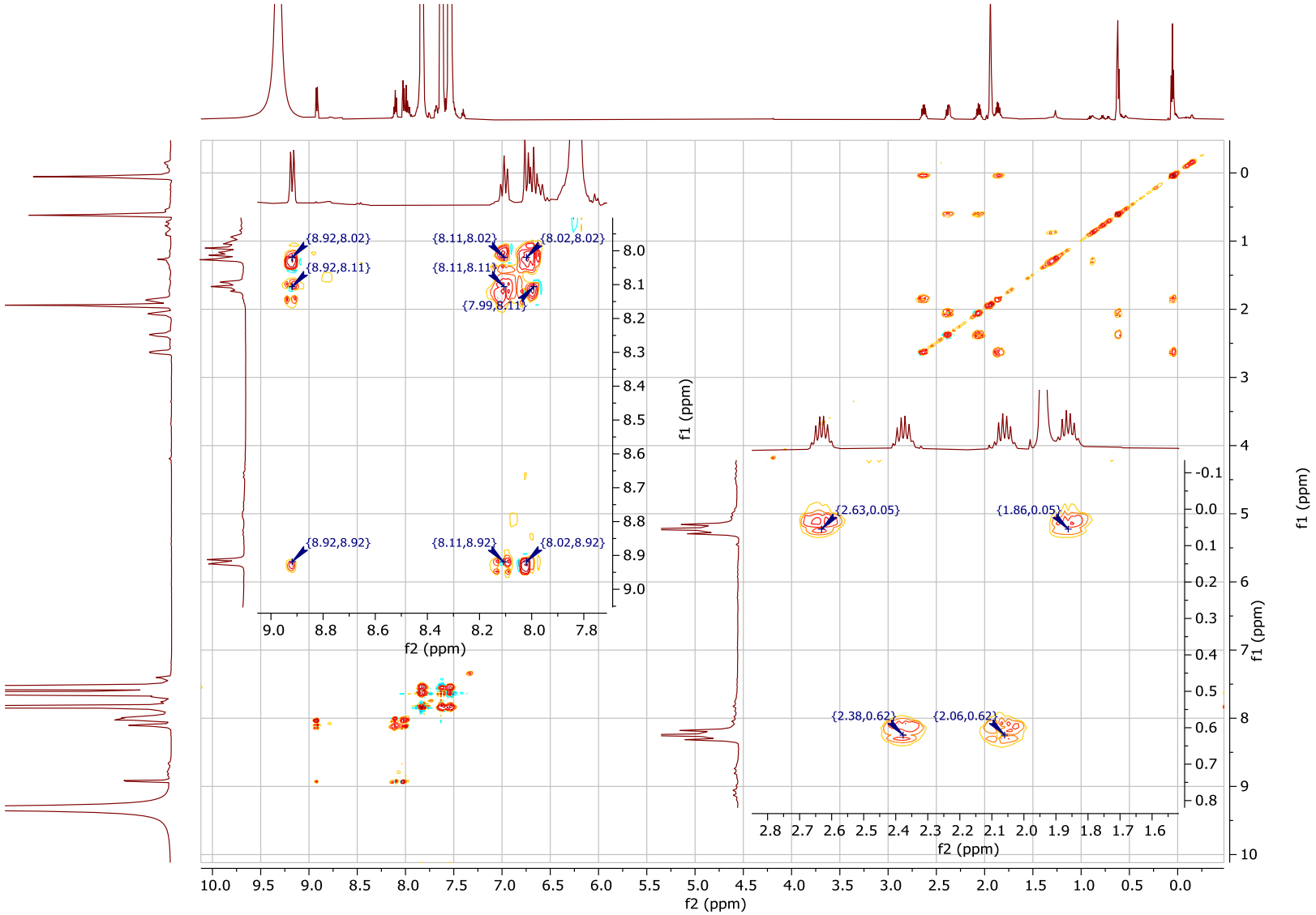

Figure S4. ^{1}H–^{1}H TOCSY spectrum of ***α,β,α,β*-P1-BSA** with expansion of areas of interest (acetonitrile-d_3, 25 °C).

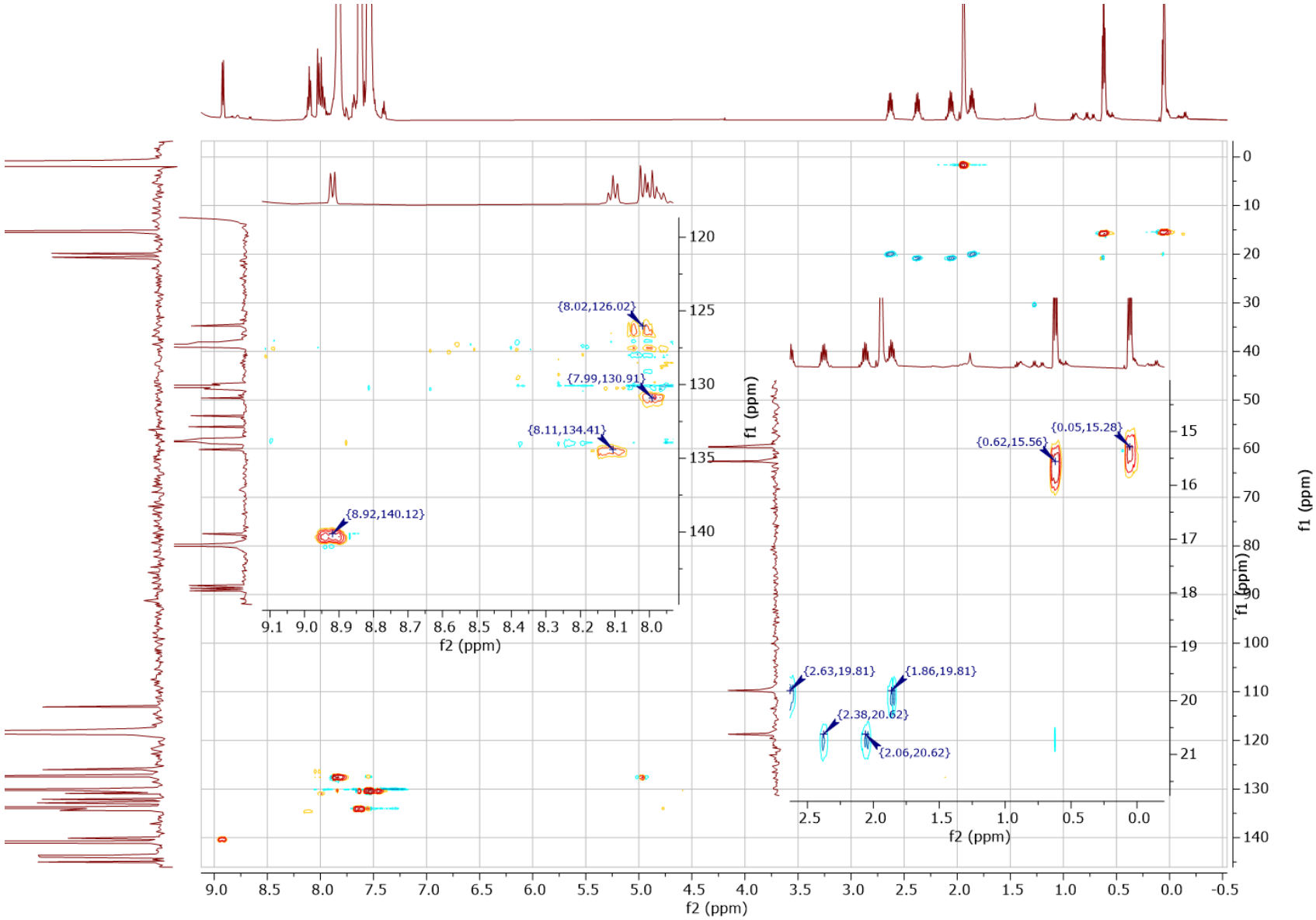

Figure S5. ^{1}H-^{13}C HSQC spectrum of *α,β,α,β*-**P1-BSA** with expansion of areas of interest (acetonitrile-d_3, 25 °C).

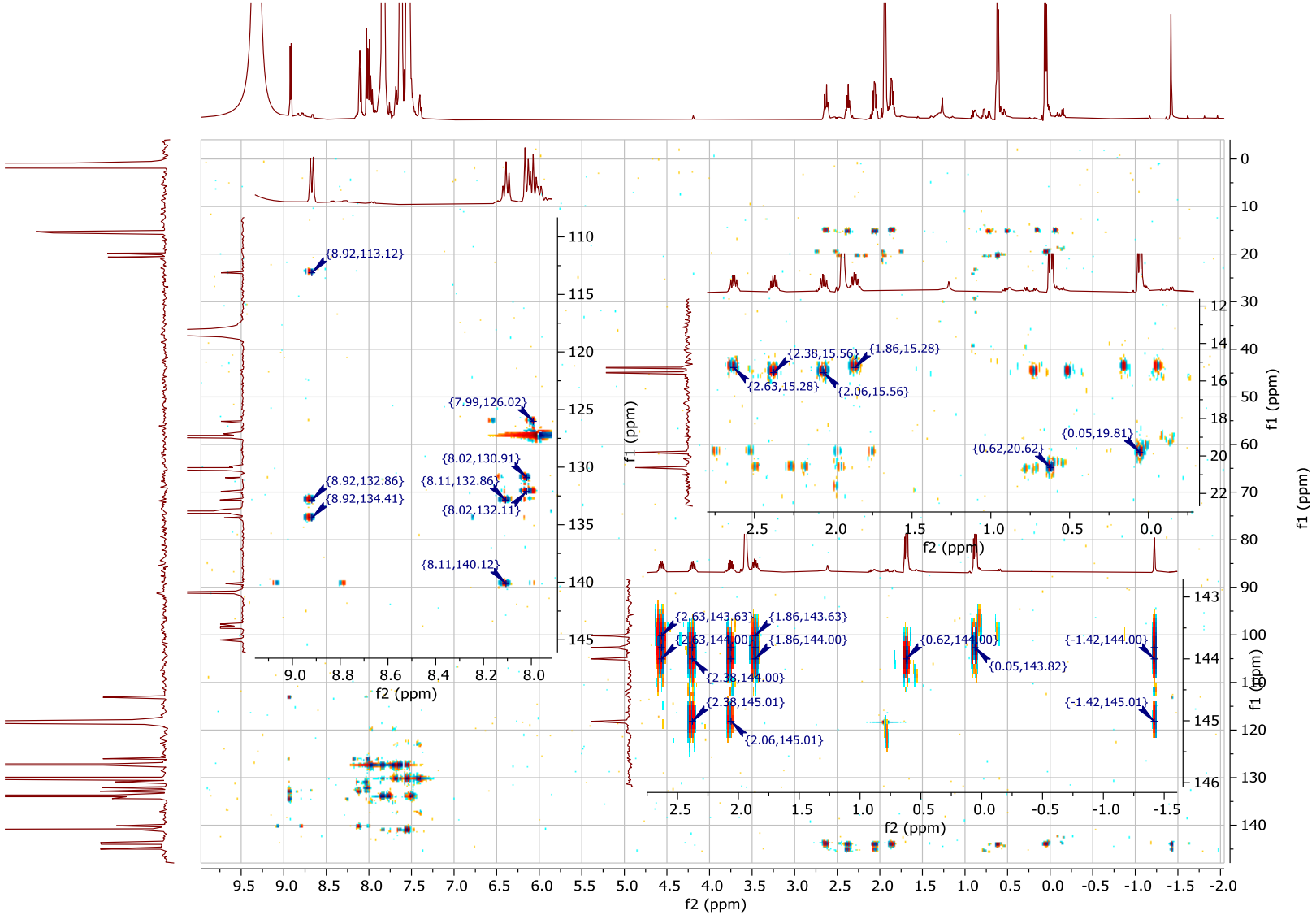

Figure S6. ^{1}H-^{13}C HMBC spectrum of *α,β,α,β*-**P1-BSA** with expansion of areas of interest (acetonitrile-d_3, 25 °C).

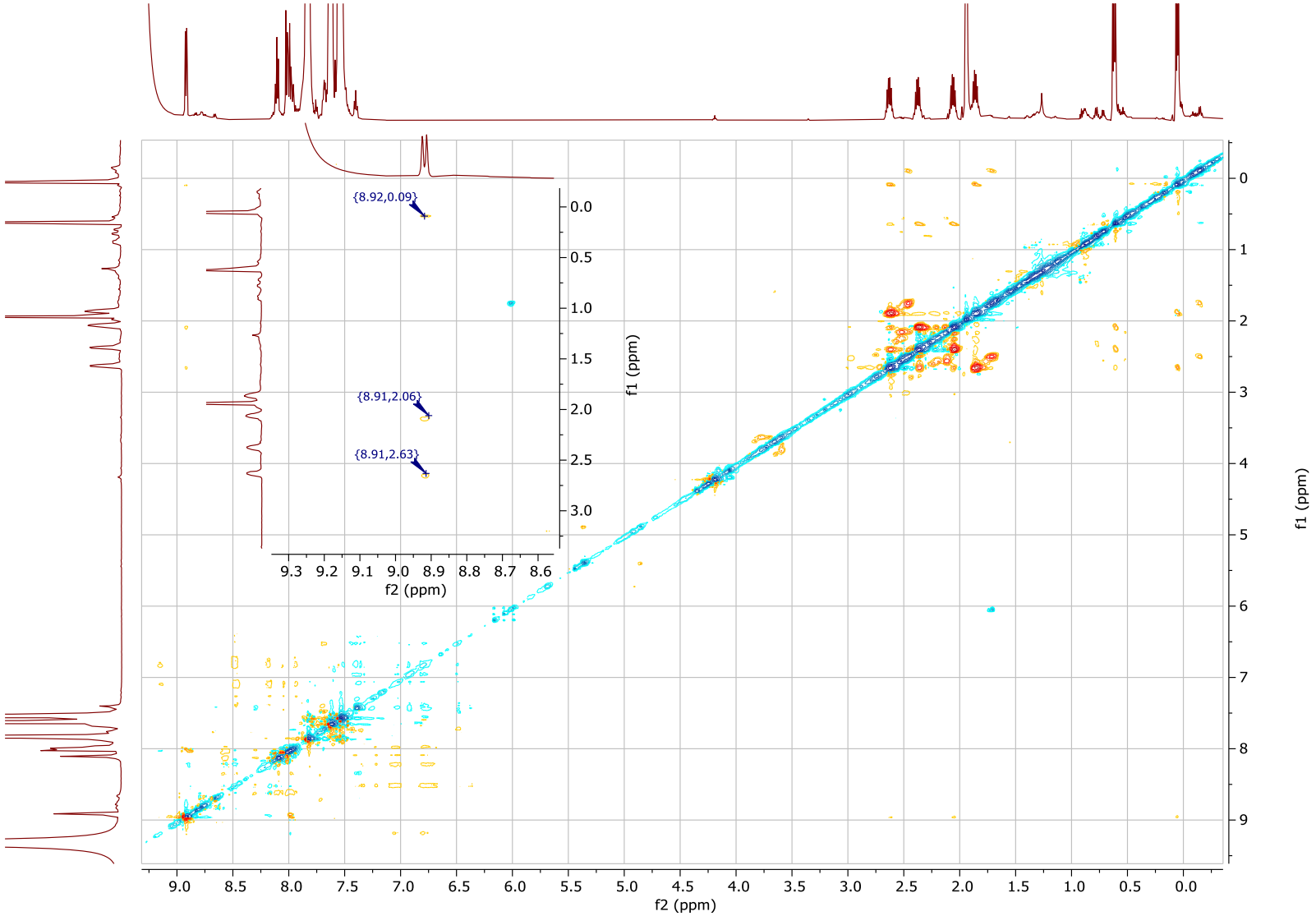

Figure S7. ^{1}H-^{1}H ROESY spectrum of *α,β,α,β*-**P1-BSA** with expansion of areas of interest (acetonitrile-d_3, 25 °C).

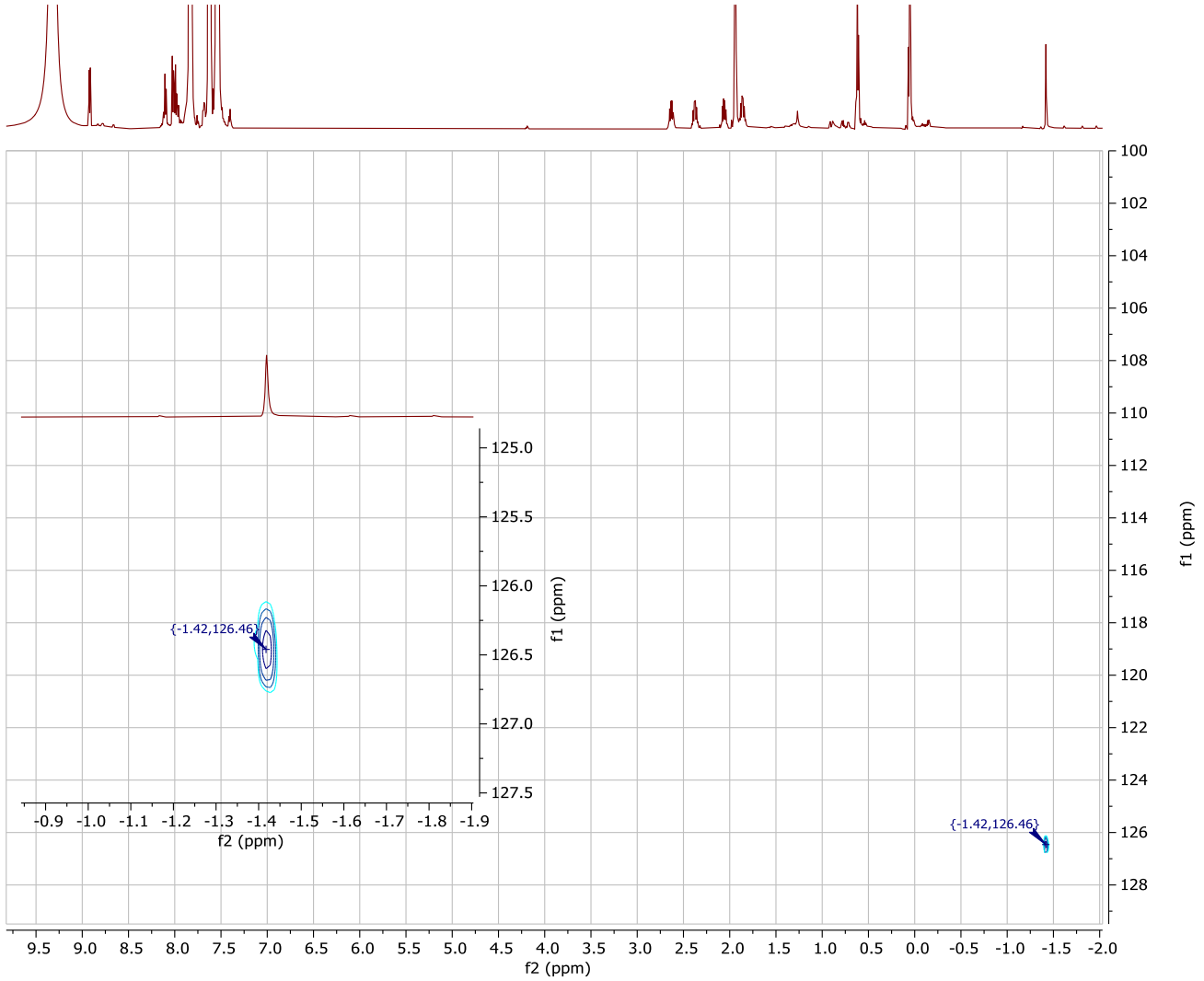

Figure S8. ^{1}H-^{15}N HSQC spectrum of *α,β,α,β*-**P1-BSA** with expansion of areas of interest (acetonitrile-d_3, 25 °C).

SUPPORTING INFORMATION

*Synthesis and Characterization of $\alpha_{2,}\beta_{2}$-**P1-BSA***

α,α,β,β-5,10,15,20-Tetrakis(2-aminiumphenyl)-2,3,7,8,12,13,17,18-octaethyl-porphyrin hexa-benzenesulfonic acid salt ($\alpha_{2,}\beta_{2}$-P1-BSA). In a sample tube benzene sulfonic acid (0.82 mg; 0.25 mmol; 50 eq.) was dissolved in 1 mL of acetonitrile-d_3. Isomerically pure α,α,β,β-5,10,15,20-tetrakis(2-aminophenyl)-2,3,7,8,12,13,17,18-octaethylporphyrinato]nickel(II) (5 mg; 0.005 mmol; 1 eq.) was added in one batch and stirred for 16 hours. The completion of demetalation followed by complex formation was identified by a distinct color change (maroon to green) of the solution. ^{1}H NMR (600 MHz, acetonitrile-d_3) δ = 8.74 (d, J = 7.4 Hz, 2H, Ar-*H* (a)), 8.66 (d, J = 7.4 Hz, 2H, Ar-*H* (b)), 8.12 (t, J = 8.0 Hz, 2H, Ar-*H* (b)), 8.08 (t, J = 7.8 Hz, 2H, Ar-*H* (a)), 8.06 (d, J = 8.0 Hz, 2H, Ar-*H* (b)), 8.03 (t, J = 7.5 Hz, 2H, Ar-*H* (b)), 7.94 (d, J = 8.1 Hz, 2H, Ar-*H* (a)), 7.90 (t, J = 8.1 Hz, 2H, Ar-*H* (a)), 2.63 (dq, J = 14.4, 7.1 Hz, 2H, C*H*$_2$ (c)), 2.50 (dq, J = 15.2, 7.6 Hz, 2H, C*H*$_2$ (a)), 2.46 (dq, J = 30.2, 15.2, 7.6 Hz, 2H, C*H*$_2$ (d)), 2.37 (dq, J = 14.7, 7.4 Hz, 2H, C*H*$_2$ (b)), 2.19 (dq, J = 14.8, 7.5 Hz, 2H, C*H*$_2$ (a)), 2.09 (dq, J = 14.7, 7.3 Hz, 2H, C*H*$_2$ (d)), 1.85 (dq, J = 14.8, 7.4 Hz, 2H, C*H*$_2$ (c)), 1.66 (dq, J = 15.0, 7.4 Hz, 2H, C*H*$_2$ (d)), 0.71 (t, J = 7.5 Hz, 6H, C*H*$_3$ (a)), 0.67 (t, J = 7.6 Hz, 6H, C*H*$_3$ (c)), -0.04 (t, J = 7.4 Hz, 6H, C*H*$_3$ (d)), -0.19 (t, J = 7.5 Hz, 6H, C*H*$_3$ (b)), -1.11 (s, 2H, N-*H* (c)), -1.40 (s, 1H, N-*H* (b)), -2.18 (s, 1H, N-*H* (a)); ^{13}C NMR (151 MHz, acetonitrile-d_3, 25 °C) δ = 145.59 (β-pyrrole (a)), 144.88 (α-pyrrole (a)), 144.65 (α-pyrrole (c)), 144.12 (α-pyrrole (d)), 143.94 (β-pyrrole (c)), 142.92 (β-pyrrole (b)), 142.76 (α-pyrrole (b)), 142.03 (β-pyrrole (d)), 140.37 (Ar (a)), 139.81 (Ar (b)), 134.19 (Ar (a)), 134.19 (Ar (b)), 133.1 (Ar (b)), 133 (Ar (a)), 132.12 (Ar (b)), 132.02 (Ar (a)), 130.63 (Ar (b)), 130.5 (Ar (a)), 126.36 (Ar (b)), 125.93 (Ar (a)), 114.85 (meso- (b)), 111.95 (meso- (a)), 20.76 (CH_2 (a)), 20.48 (CH_2 (c)), 19.1 (CH_2 (b)), 19.1 (CH_2 (d)), 15.92 (CH_3 (b)), 15.87 (CH_3 (d)), 15.37 (CH_3 (a)),15.19 (CH_3 (c)) ppm.; ^{15}N NMR (61 MHz, acetonitrile-d_3) δ = 125.84 (N-H (c)), 127.23(N-H (b)), 126.94 (N-H (a)) ppm.

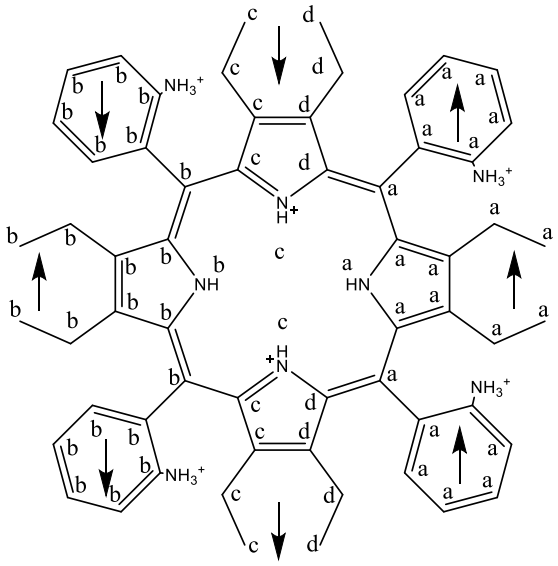

Figure S9. Structure of $\alpha_{2,}\beta_{2}$-**P1-BSA** highlighting the positions used in NMR characterizations.

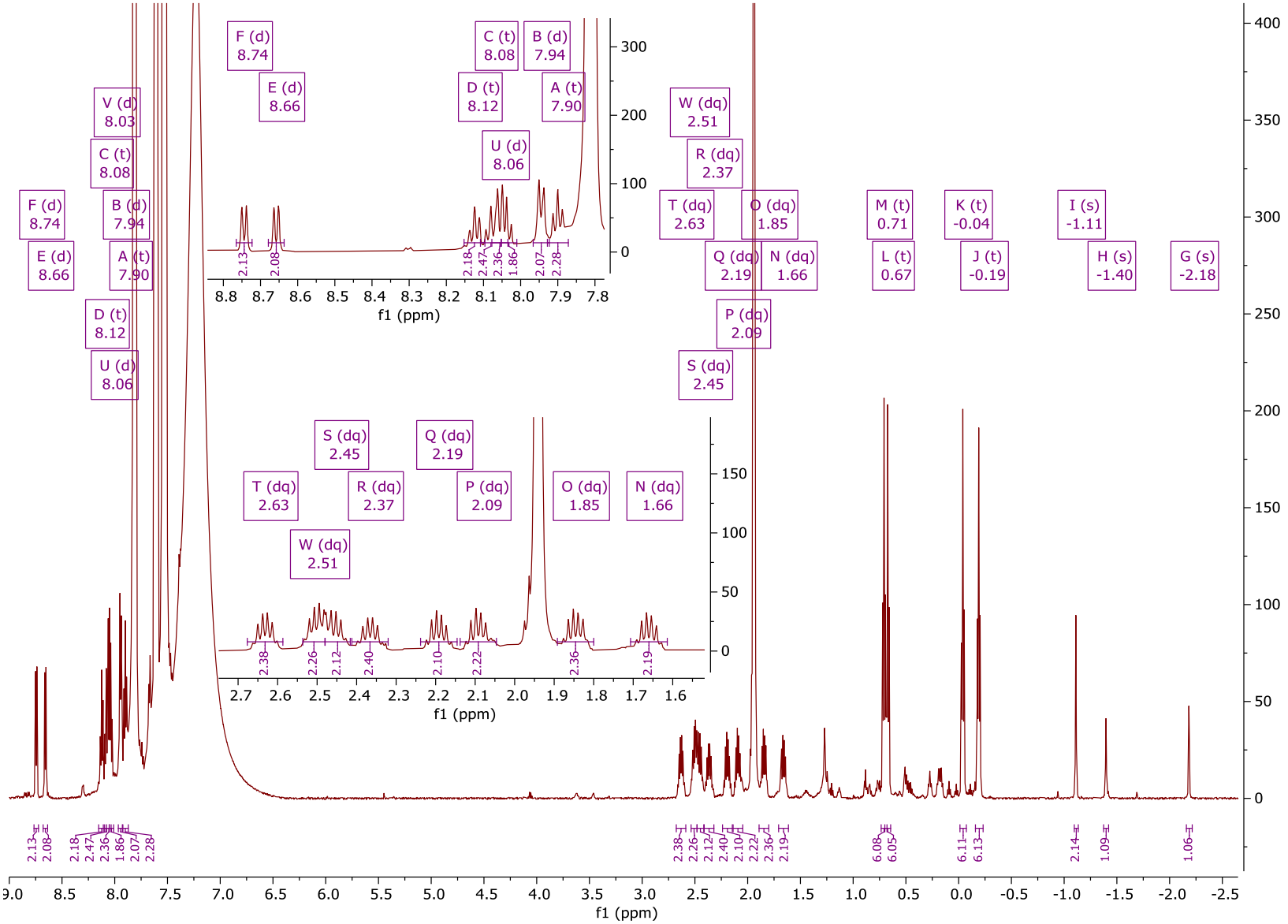

Figure S10. ^{1}H NMR spectrum of $\alpha_{2,}\beta_{2}$-**P1-BSA** with expansion of areas of interest (600 MHz, acetonitrile-d_3, 25 °C).

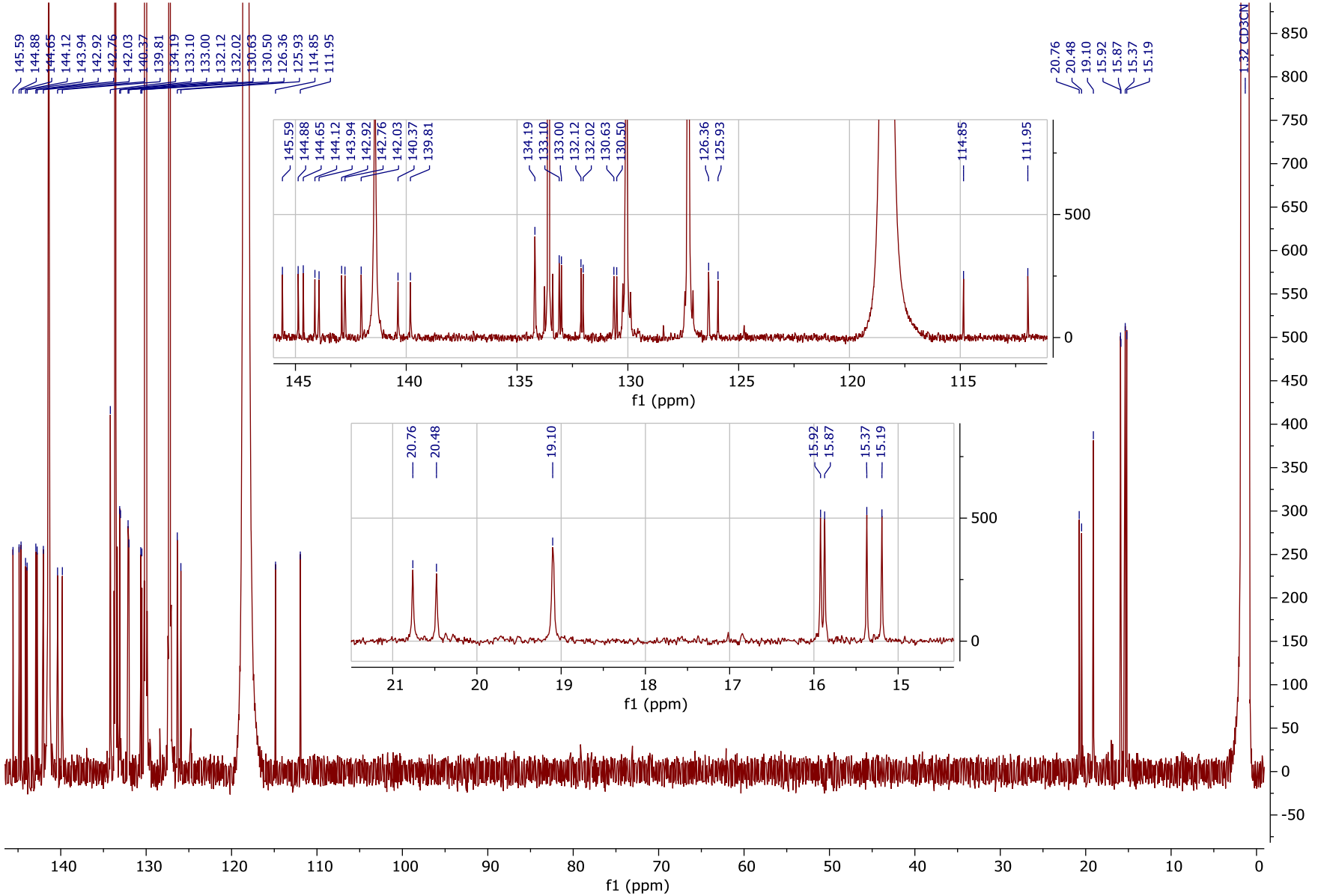

Figure S11. ^{13}C NMR spectrum of α_2,β_2-**P1-BSA** with expansion of areas of interest (151 MHz, acetonitrile-d_3, 25 °C).

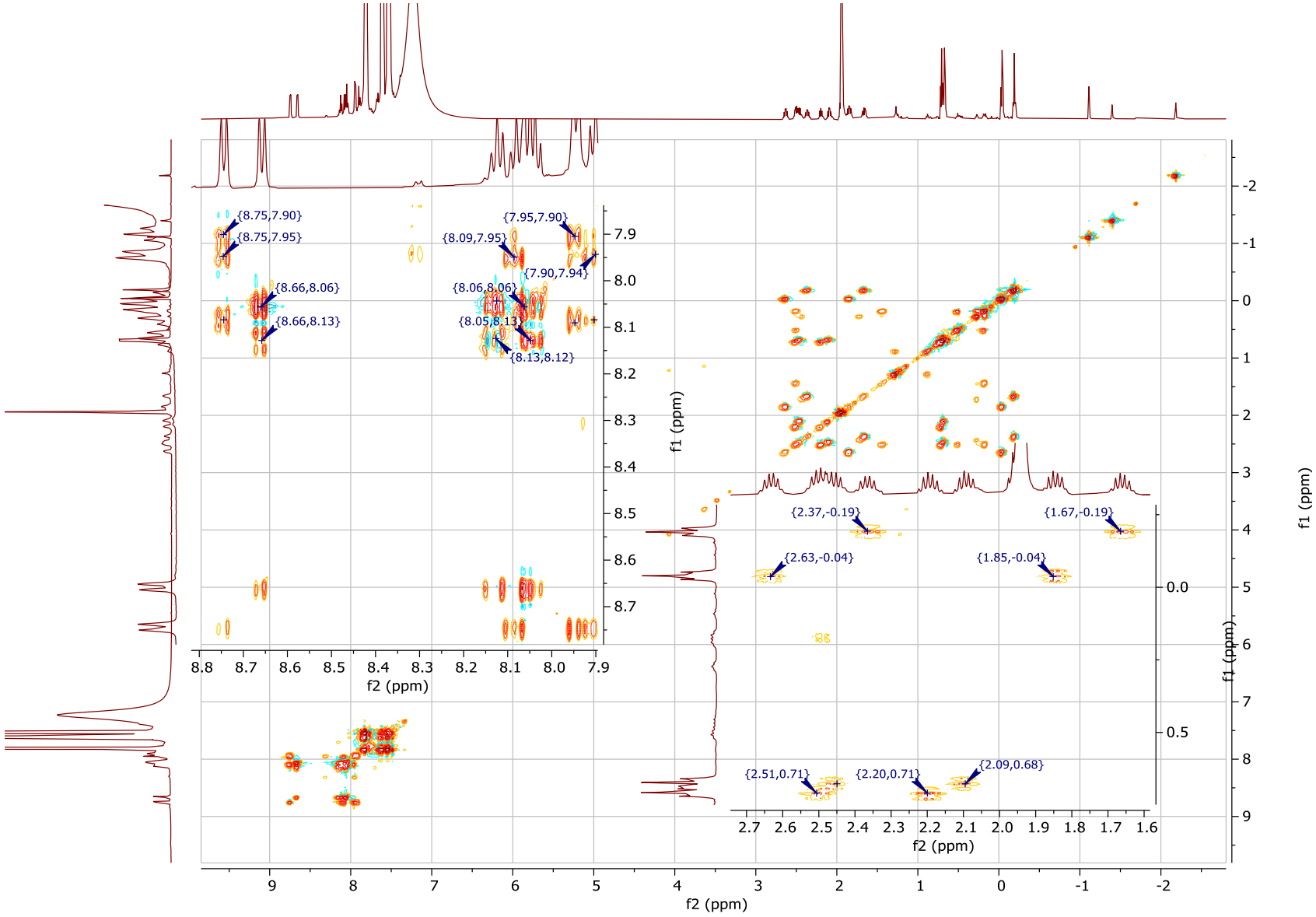

Figure S12. ^{1}H–^{1}H TOCSY spectrum of α_2,β_2-**P1-BSA** with expansion of areas of interest (acetonitrile-d_3, 25 °C).

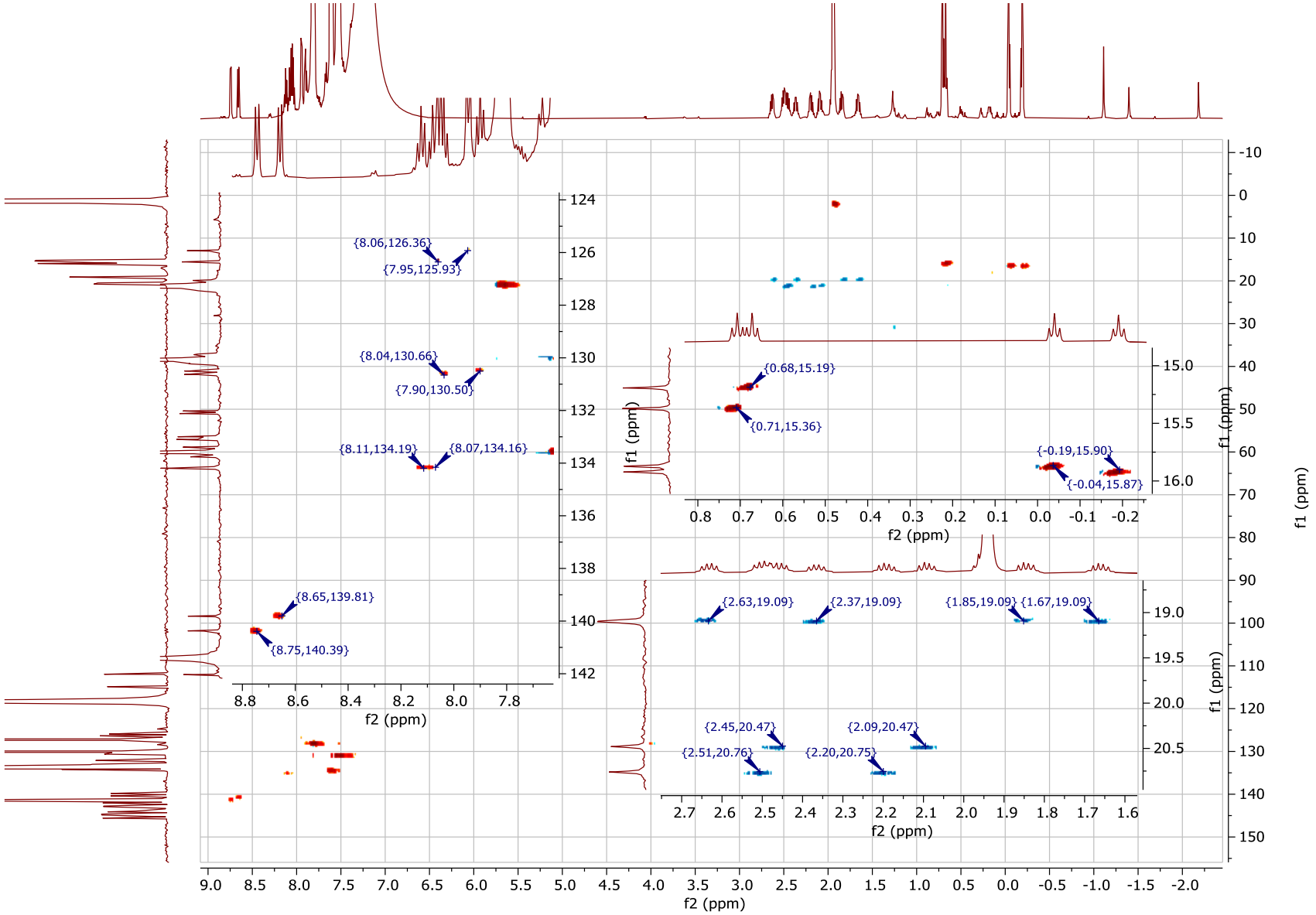

Figure S13. ^{1}H-^{13}C HSQC spectrum of α_2,β_2-**P1-BSA** with expansion of areas of interest (acetonitrile-d_3, 25 °C).

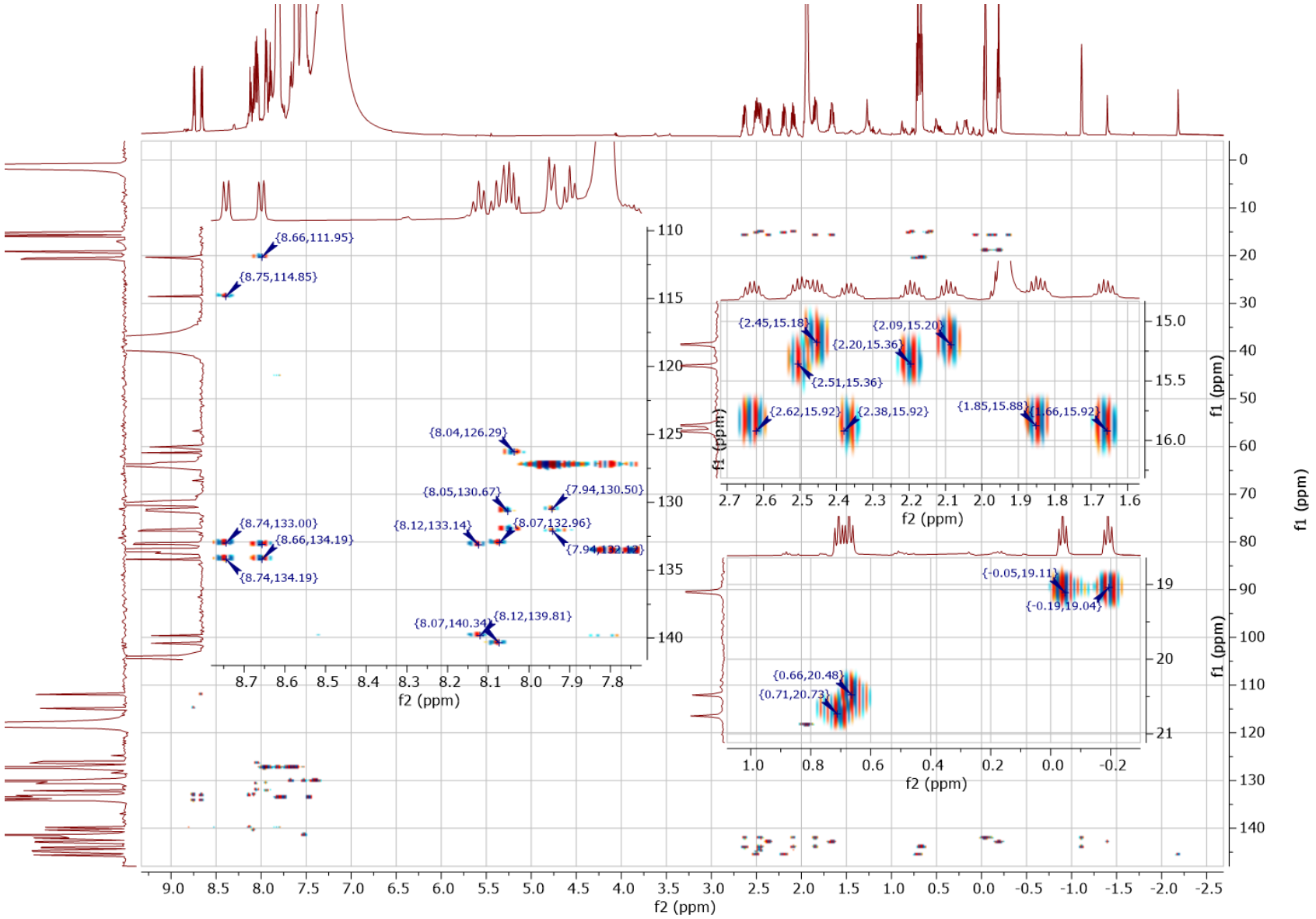

Figure S14. ^{1}H-^{13}C HMBC spectrum of $\alpha_{2,}\beta_{2}$-**P1-BSA** with expansion of areas of interest (acetonitrile-d_3, 25 °C).

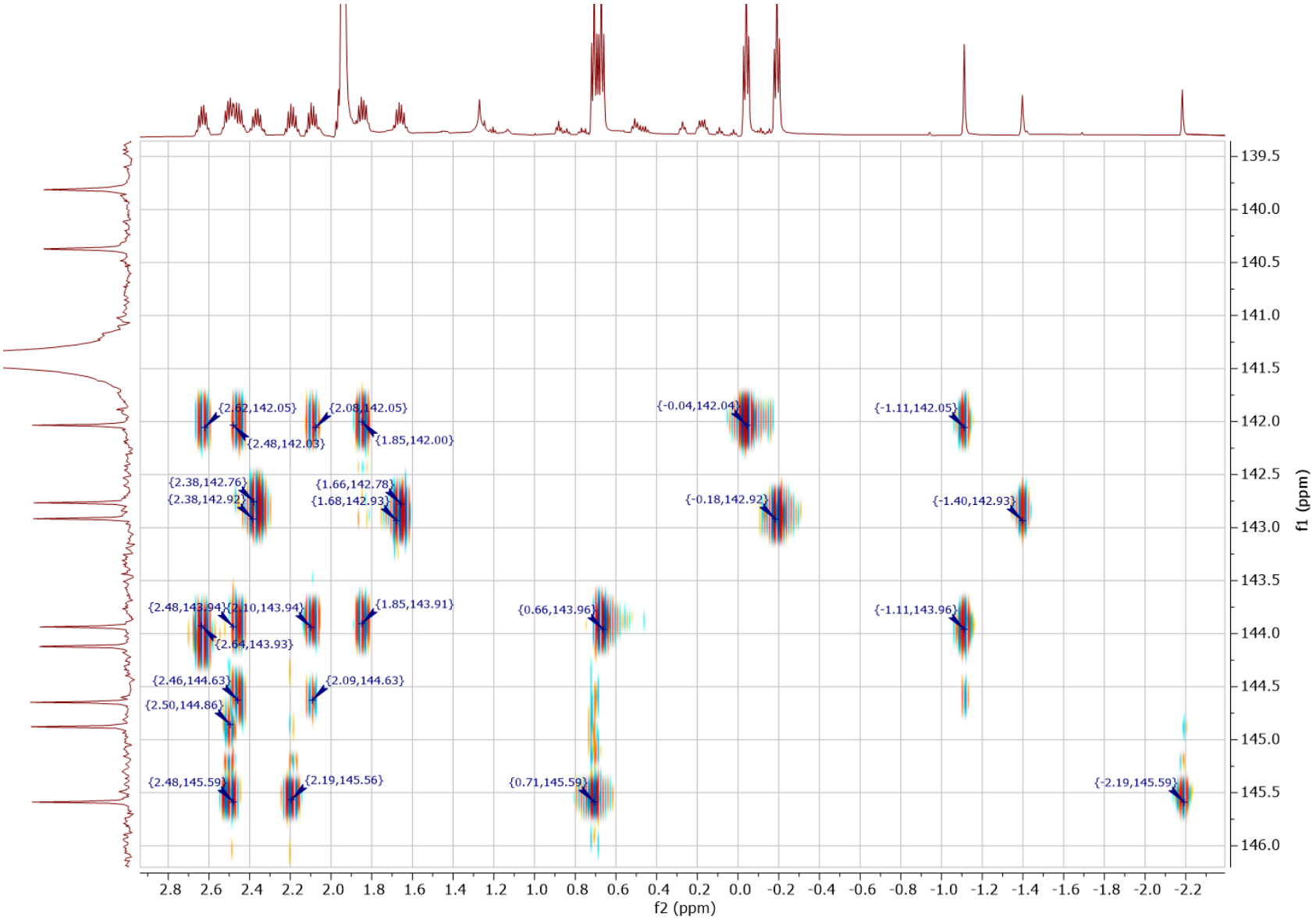

Figure S15. ^{1}H-^{13}C HMBC spectrum, expansion of area of interest of α_2,β_2-**P1-BSA** (acetonitrile-d_3, 25 °C).

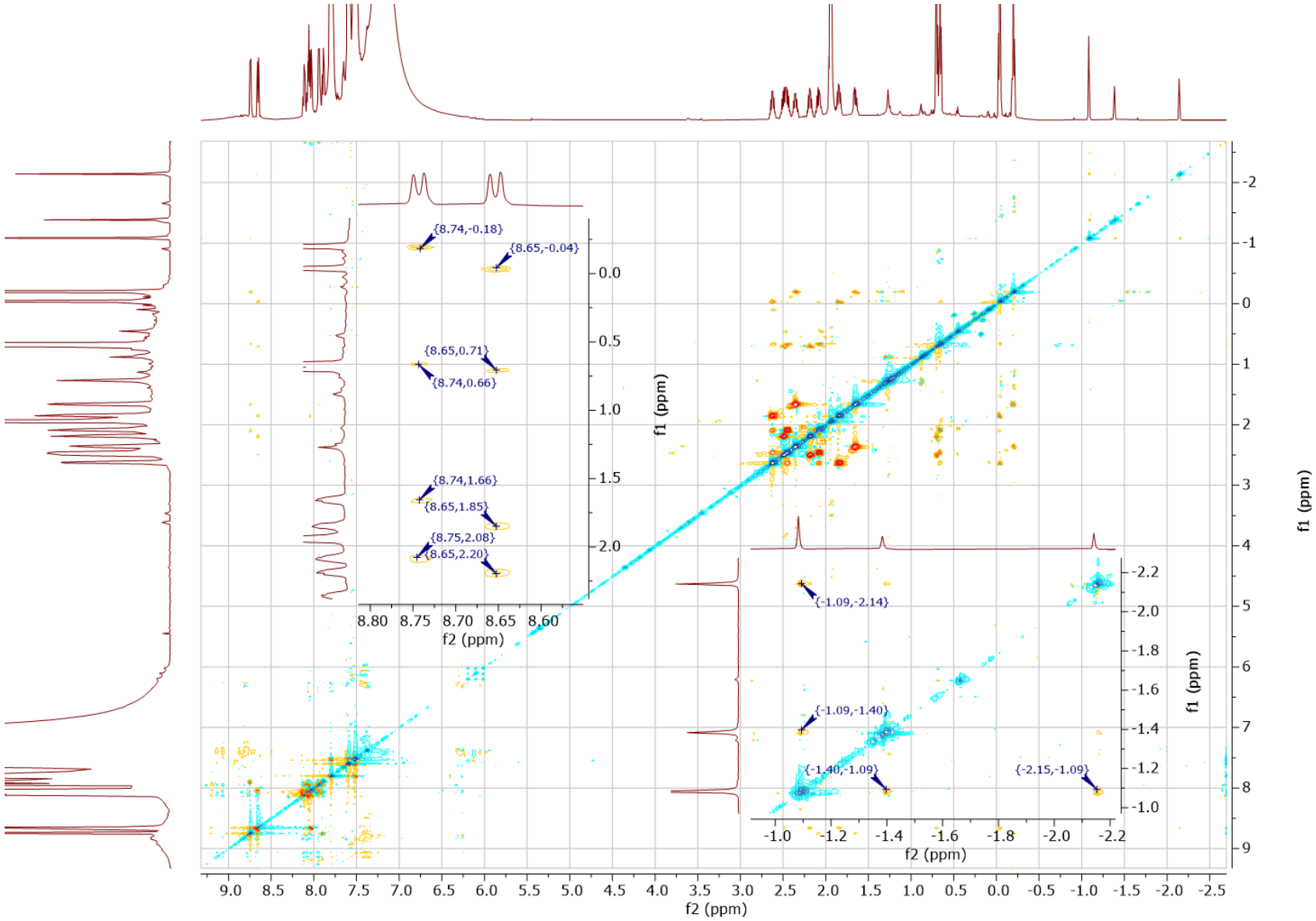

Figure S16. ^{1}H-^{1}H ROESY spectrum of α_2,β_2-**P1-BSA** with expansion of areas of interest (acetonitrile-d_3, 25 °C).

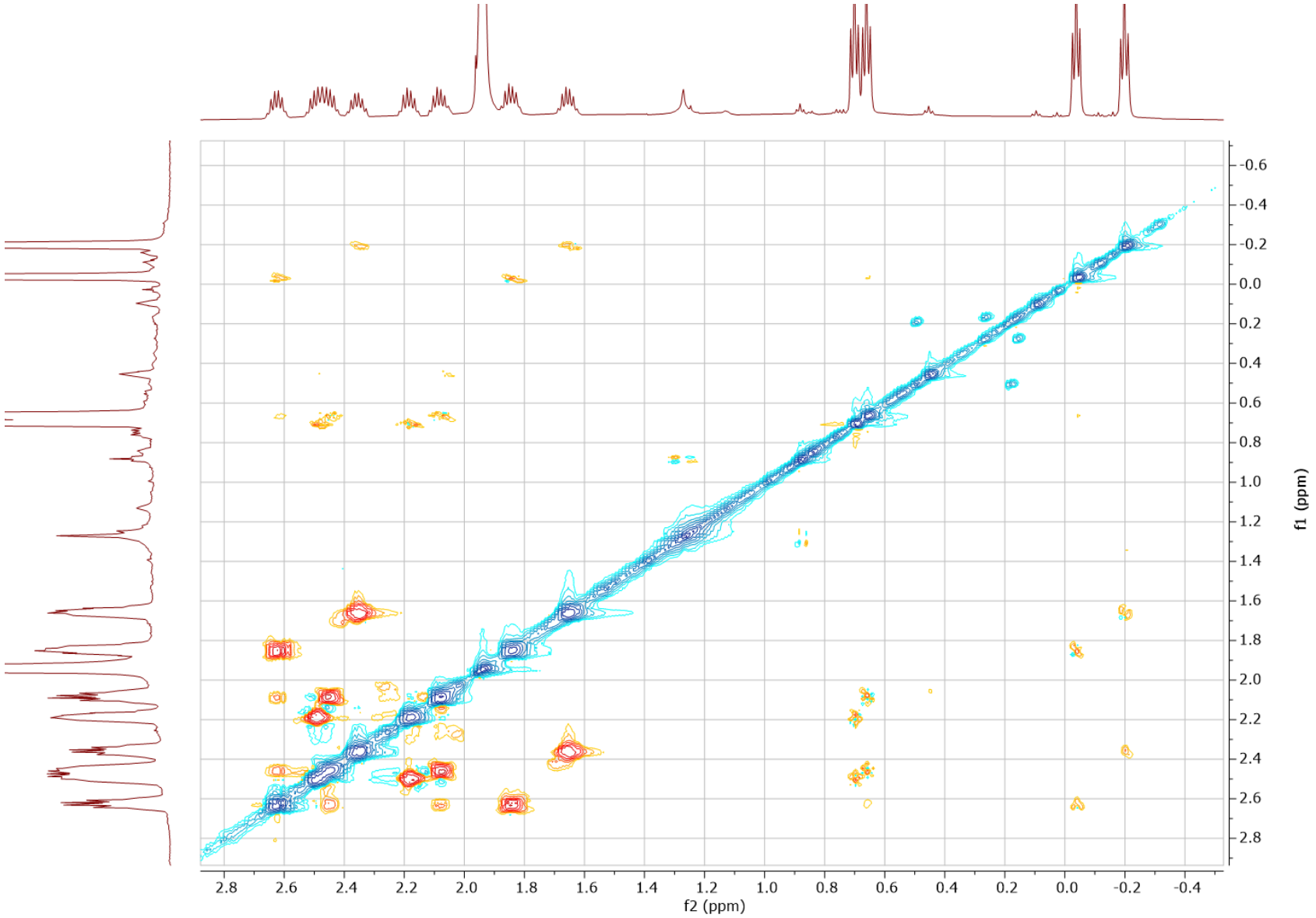

Figure S17. ^{1}H-^{1}H ROESY spectrum of α_{2},β_{2}-**P1-BSA**, expansion of aliphatic area (acetonitrile-d_3, 25 °C).

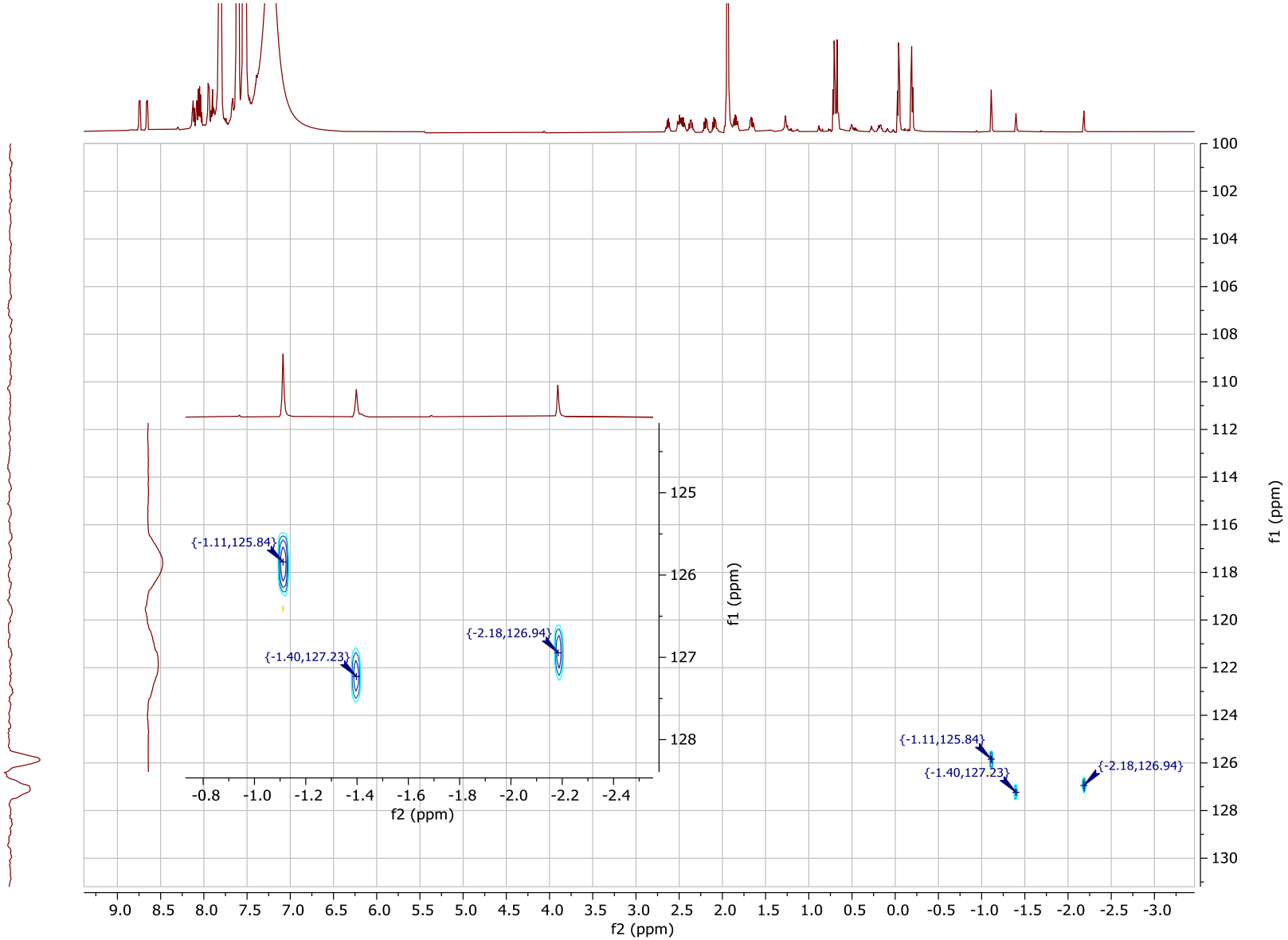

Figure S18. ^{1}H-^{15}N HSQC spectrum of α_2,β_2-**P1-BSA** with expansion of areas of interest (acetonitrile-d_3, 25 °C).

SUPPORTING INFORMATION

*Synthesis and Characterization of α_3,β-**P1-BSA***

α,α,α,β-5,10,15,20-Tetrakis(2-aminiumphenyl)-2,3,7,8,12,13,17,18-octaethyl-porphyrin hexa-benzenesulfonic acid salt (α_3,β-P1-BSA). In a sample tube benzene sulfonic acid (0.82 mg; 0.25 mmol; 50 eq.) was dissolved in 1 mL of acetonitrile-d3. Isomerically pure [α,β,β,β-5,10,15,20-tetrakis(2-aminophenyl)-2,3,7,8,12,13,17,18-octaethylporphyrinato]nickel(II) (5 mg; 0.005 mmol; 1 eq.) was added in one batch and stirred for 16 hours. The completion of demetalation followed by complex formation was identified by a clear color change (maroon to green) of the solution. During slow evaporation, green/blue shard habit crystals were formed. ^{1}H NMR (600 MHz, acetonitrile-d_3) δ = 8.85 (d, *J* = 7.3 Hz, 1H, Ar-*H* (d)), 8.83 (d, *J* = 7.5 Hz, 1H, Ar-*H* (a)), 8.72 (d, *J* = 7.4 Hz, 1H, Ar-*H* (c)), 8.62 (d, *J* = 7.5 Hz, 1H, Ar-*H* (b)), 8.14 – 8.07 (m, 2H, Ar-*H* (a,b,c,d), 8.08 – 7.97 (m, 6H, Ar-*H* (b,c)), 7.96 (d, *J* = 4.8 Hz, 1H, Ar-*H* (d)), 7.94 (d, *J* = 4.8 Hz, 1H, Ar-*H* (a)),7.89 (t, *J* = 7.5 Hz, 1H, Ar-*H* (d)), 7.85 (t, *J* = 7.5 Hz, 1H, Ar-*H* (a)), 2.61 (dq, *J* = 14.8, 7.4 Hz, 2H, C*H*$_2$ (a,f)), 2.52 (dq, *J* = 15.3, 7.6 Hz, 1H, C*H*$_2$ (g)), 2.44 (ddq, *J* = 21.3, 14.2, 7.4 Hz, 4H, C*H*$_2$ (a,b,h,e)), 2.21 (ddq, *J* = 30.1, 15.1, 7.6 Hz, 2H, C*H*$_2$ (g,d)), 2.10 – 1.99 (m, 3H, C*H*$_2$ (d,e,h)), 1.85 (dq, *J* = 15.1, 7.5 Hz, 2H, C*H*$_2$ (f,c)), 1.70 (dq, *J* = 15.8, 8.0 Hz, 2H, C*H*$_2$ (a.b)), 0.74 (t, *J* = 7.5 Hz, 3H, C*H*$_3$ (d)), 0.71 (t, *J* = 7.5 Hz, 3H, C*H*$_3$ (g)), 0.45 (t, *J* = 7.5 Hz, 3H, C*H*$_3$ (h)), 0.42 (t, *J* = 7.5 Hz, 3H, C*H*$_3$ (e)), 0.10 (t, *J* = 7.4 Hz, 3H, C*H*$_3$ (f)), 0.02 (t, *J* = 7.4 Hz, 3H, C*H*$_3$ (c)), -0.11 (t, *J* = 7.5 Hz, 3H, C*H*$_3$ (a)), -0.16 (t, *J* = 7.5 Hz, 3H, C*H*$_3$ (b)), -0.89 (s, 1H, N-*H* (d)), -1.25 (s, 1H, N-*H* (c)), -1.37 (s, 1H, N-*H* (a)), -1.61 (s, 1H, N-*H* (b)) ppm.; ^{13}C NMR (151 MHz, acetonitrile-d_3) δ = 145.59 (α-pyrrole (h)), 145.29 (β-pyrrole (d)), 145.04 (α-pyrrole (d)), 144.88 (α-pyrrole (g)), 144.71 (β-pyrrole (g)), 144.26 (α-pyrrole (e)), 143.95 (α-pyrrole (c)), 143.76 (β-pyrrole (h)), 143.69 (α-pyrrole (f)), 143.4 (β-pyrrole (e)), 143.4 (α-pyrrole (a)), 143.27 (β-pyrrole (a)), 143.26 (β-pyrrole (c)), 142.9 (β-pyrrole (f)), 142.65 (α-pyrrole (b)), 141.95 (β-pyrrole (b)), 140.84 (Ar (a)), 140.43 (Ar (b)), 140.21 (Ar (c)), 139.35 (Ar (d)), 134.21 (Ar (b)), 134.14 (Ar (c)), 134.14 (Ar (a)), 134.05 (Ar (d)), 133.47 (Ar (d)), 133.11 (Ar (c)), 133.07 (Ar (b)), 133.04 (Ar (a)), 132.22 (Ar (d)), 132.22 (Ar (b)), 131.89 (Ar (a)), 131.86 (Ar (c)), 130.7 (Ar (c)), 130.61 (Ar (a)), 130.51 (Ar (b)), 130.43 (Ar (d)), 126.13 (Ar (c)), 126.05 (Ar (d)), 126.05 (Ar (b)), 125.81 (Ar (a)), 114.9 (meso- (a)), 113.39 (meso- (d)), 113.36 (meso- (b)), 111.53 (meso- (c)), 20.69 (CH_2 (d)), 20.58 (CH_2 (g)), 20.23 (CH_2 (h)), 20.23 (CH_2 (e)), 19.53 (CH_2 (f)), 19.53 (CH_2 (c)), 19.34 (CH_2 (a)), 8.99 (CH_2 (b)), 15.96 (CH_3 (b)), 15.84 (CH_3 (f)), 15.72 (CH_3 (a)), 15.67 (CH_3 (h)), 15.57 (CH_3 (d)), 15.29 (CH_3 (g)), 15.28 (CH_3 (c)), 15.26 (CH_3 (e)) ppm.; ^{15}N NMR (61 MHz, acetonitrile-d_3) δ = 127.27 (N-H (d)), 127.04 (N-H (c)), 125.90(N-H (a)), 126.88 (N-H (b)).

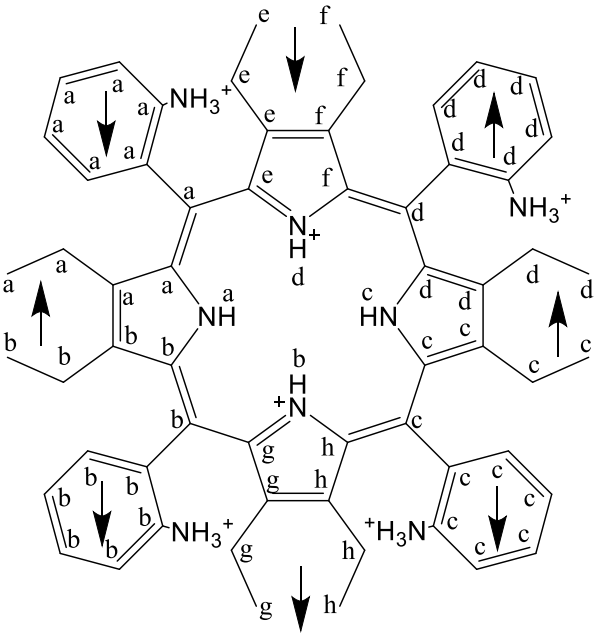

Figure S19. Structure of α_3,β-**P1-BSA** highlighting the positions used in NMR characterizations.

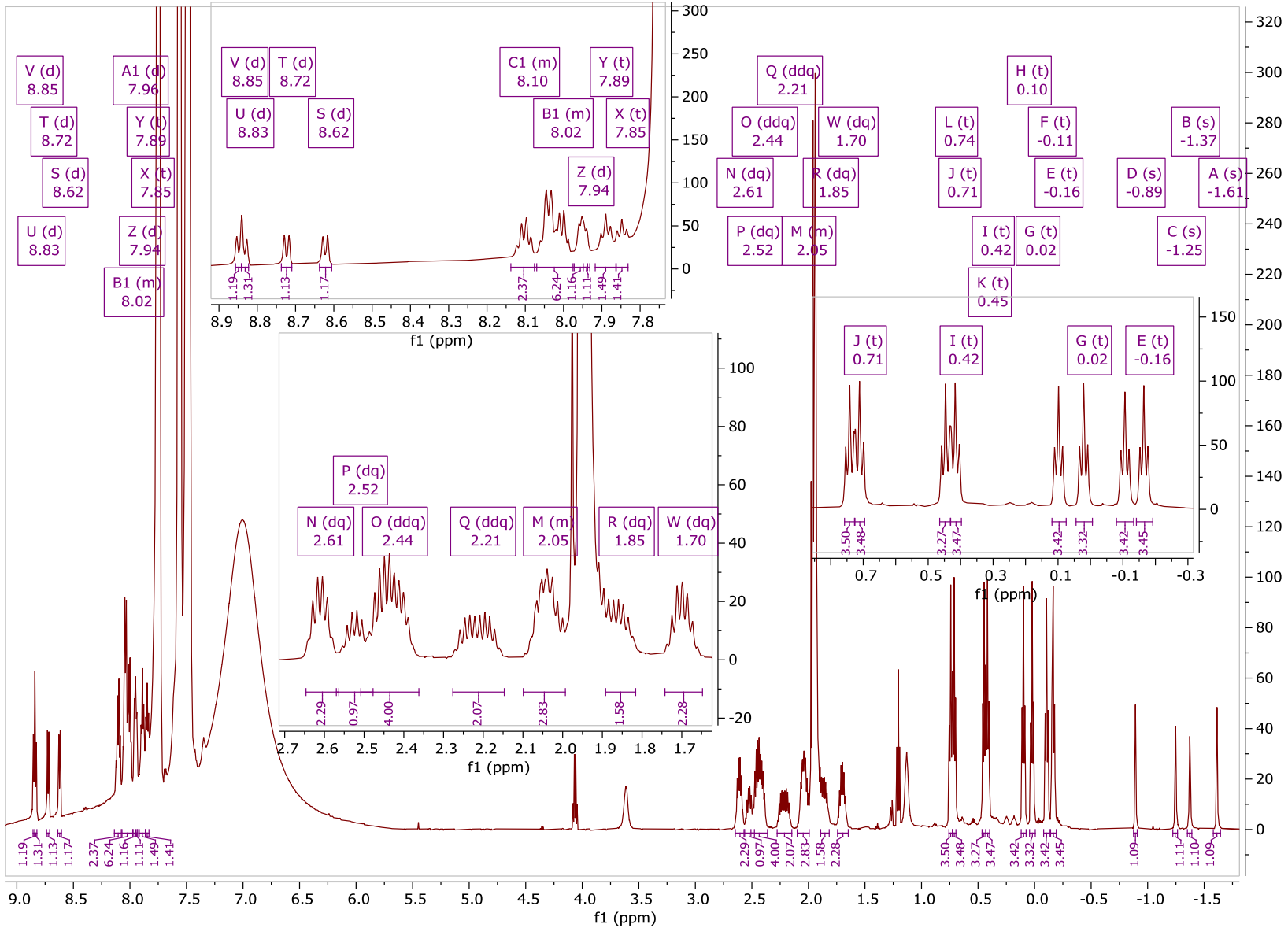

Figure S20. ^{1}H NMR spectrum of $\alpha_{3,}\beta$-**P1-BSA** with expansion of areas of interest (600 MHz, acetonitrile-d_3, 25 °C).

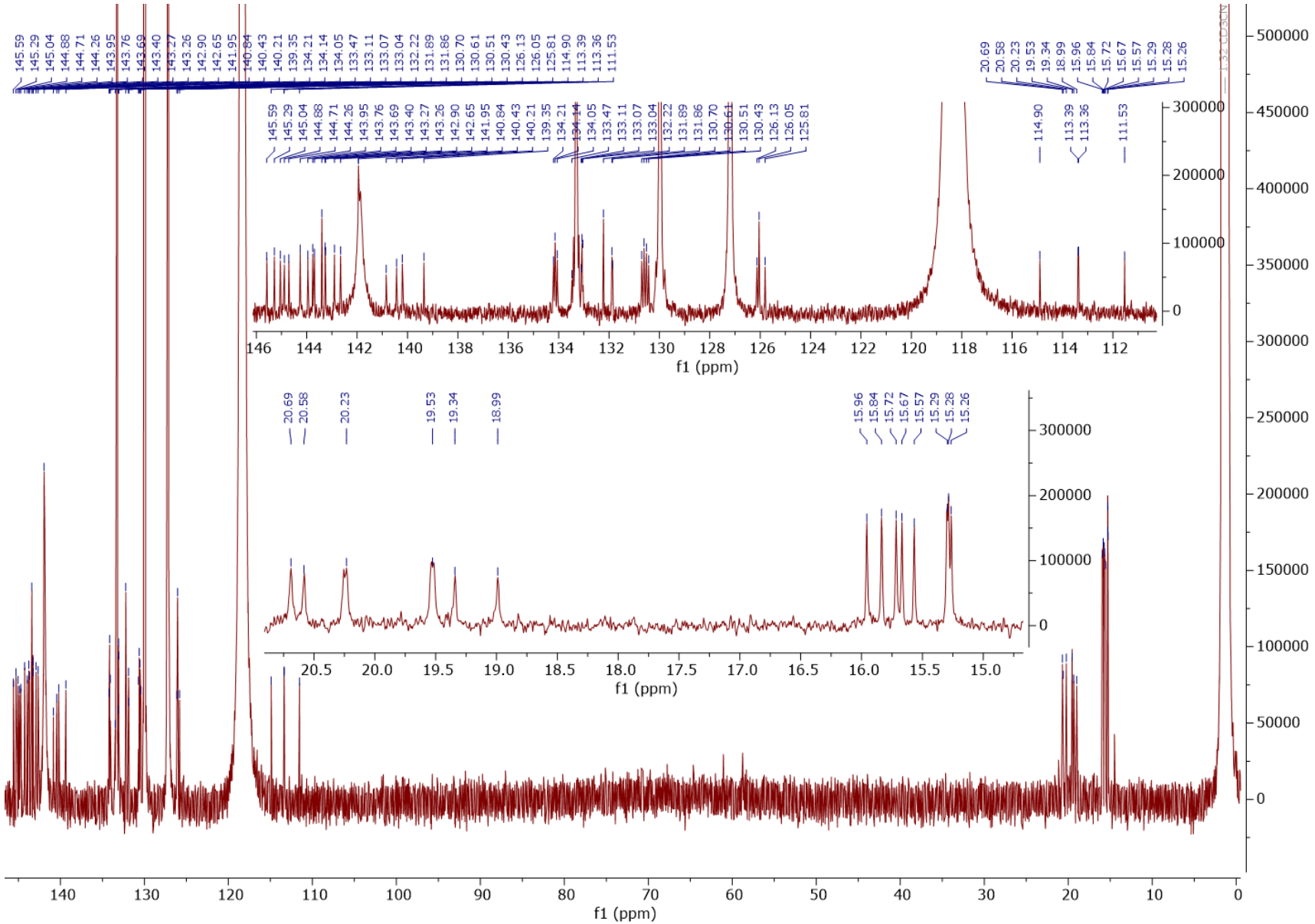

Figure S21. ^{13}C NMR spectrum of α_3,β-**P1-BSA** with expansion of areas of interest (151 MHz, acetonitrile-d_3, 25 °C).

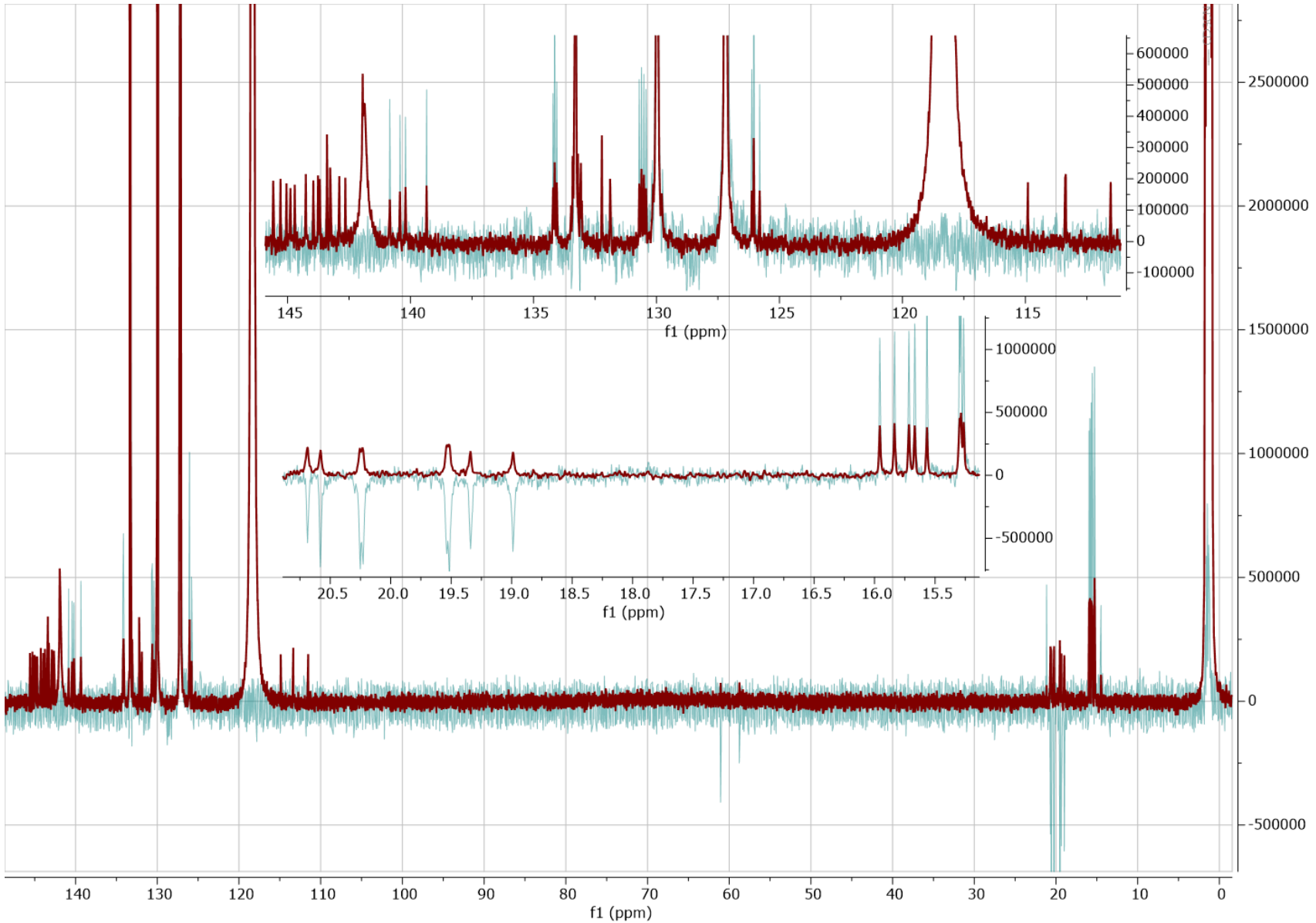

Figure S22. ^{13}C NMR and DEPT-135 overlay spectra of α_3,β-**P1-BSA** with expansion of areas of interest (151 MHz, acetonitrile-d_3, 25 °C).

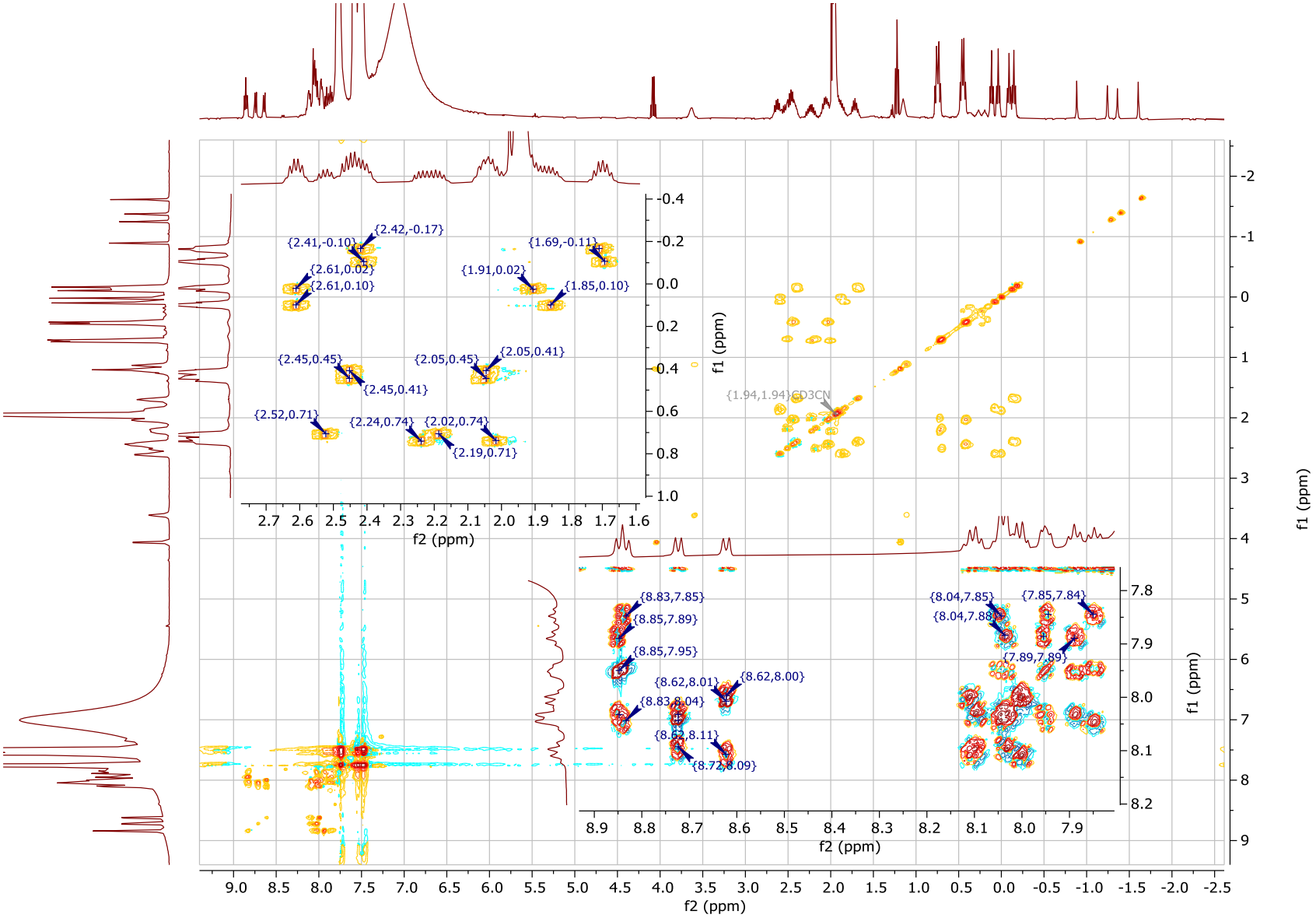

Figure S23. ^{1}H–^{1}H TOCSY spectrum of $\alpha_{3,}\beta$-**P1-BSA** with expansion of areas of interest (acetonitrile-d_3, 25 °C).

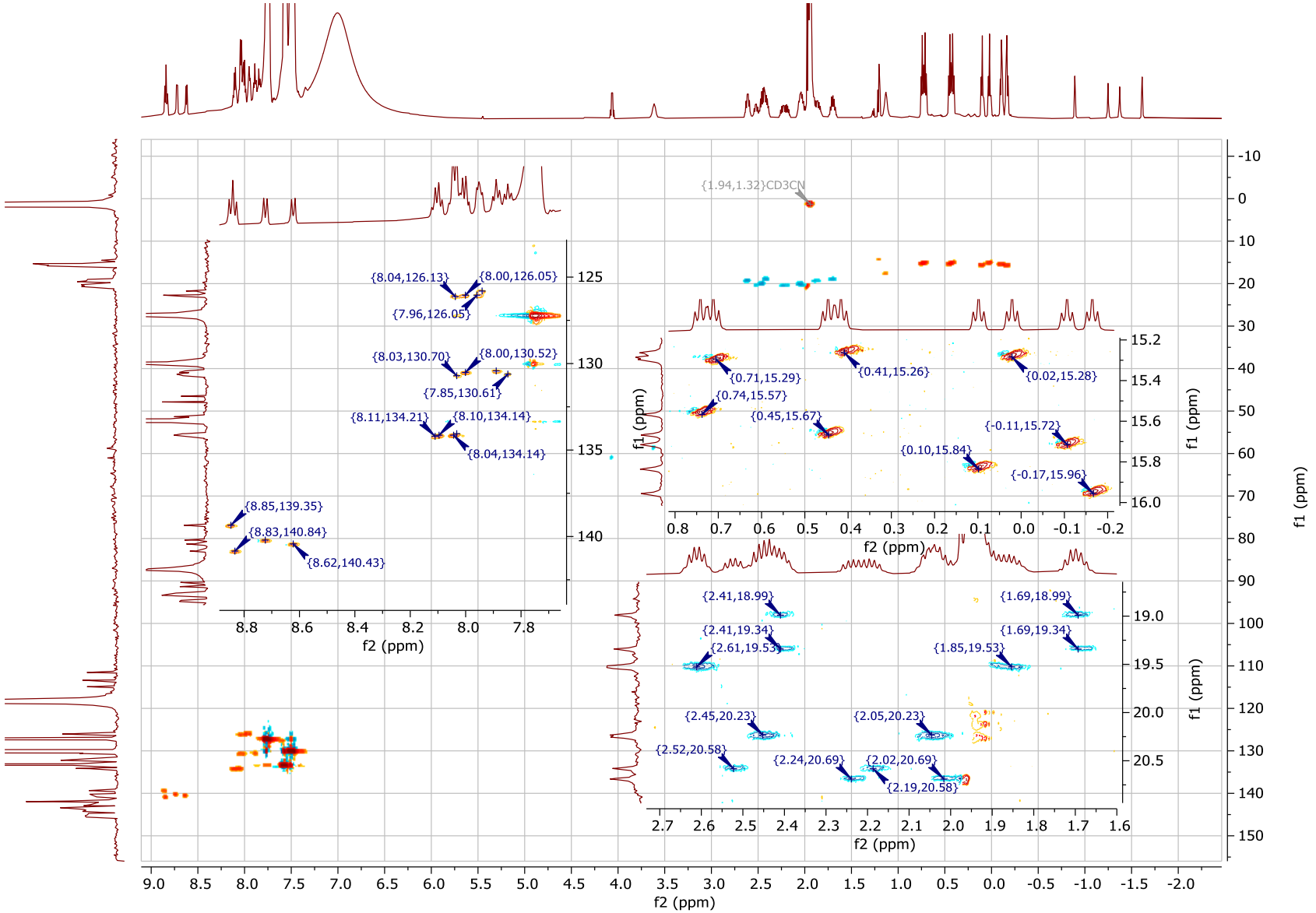

Figure S24. ^{1}H-^{13}C HSQC spectrum of *α*$_{3,}$*β*-**P1-BSA** with expansion of areas of interest (acetonitrile-*d*$_3$, 25 °C).

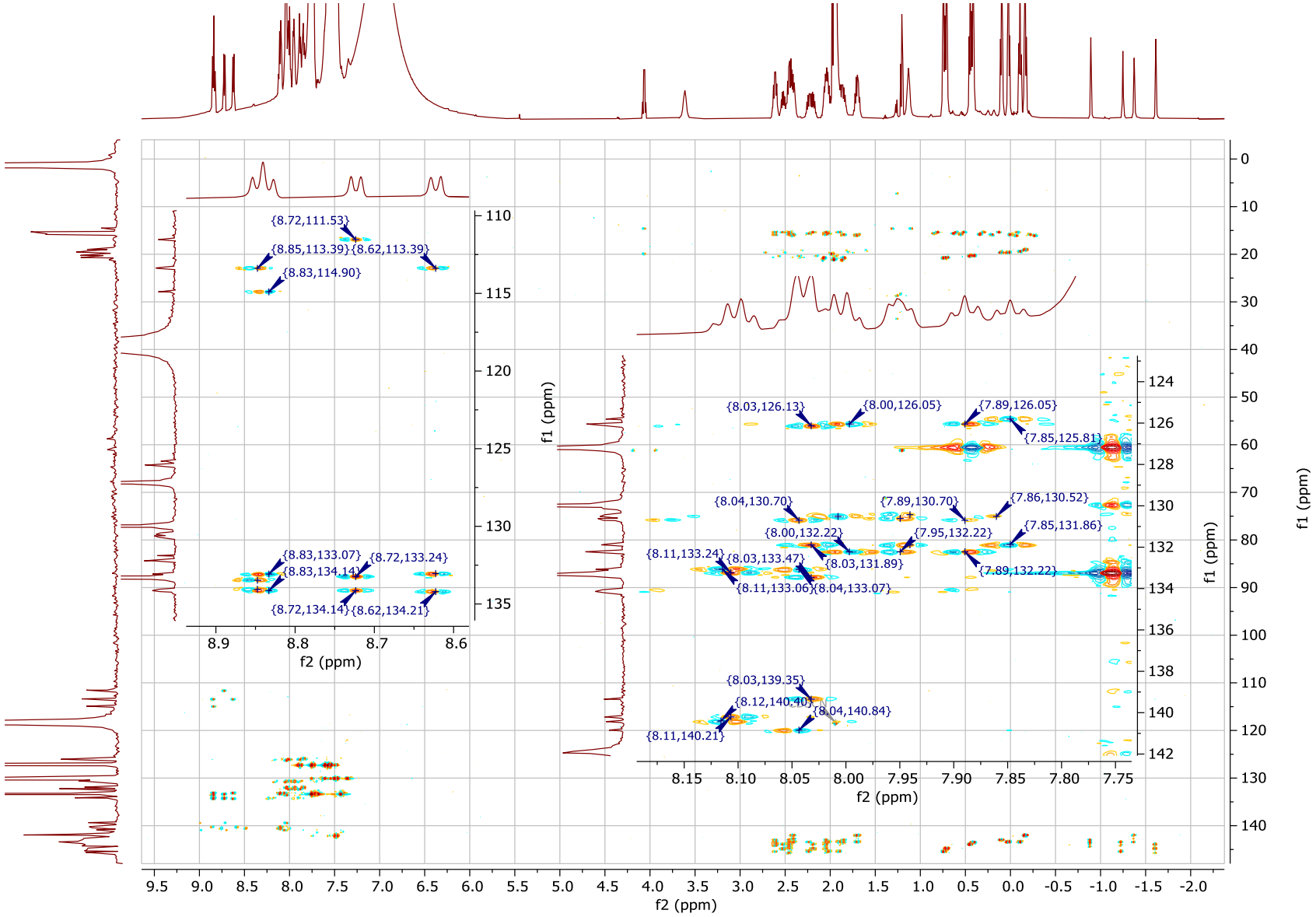

Figure S25. ^{1}H-^{13}C HMBC spectrum of $\alpha_{3,}\beta$-**P1-BSA** with expansion of areas of interest (acetonitrile-d_3, 25 °C).

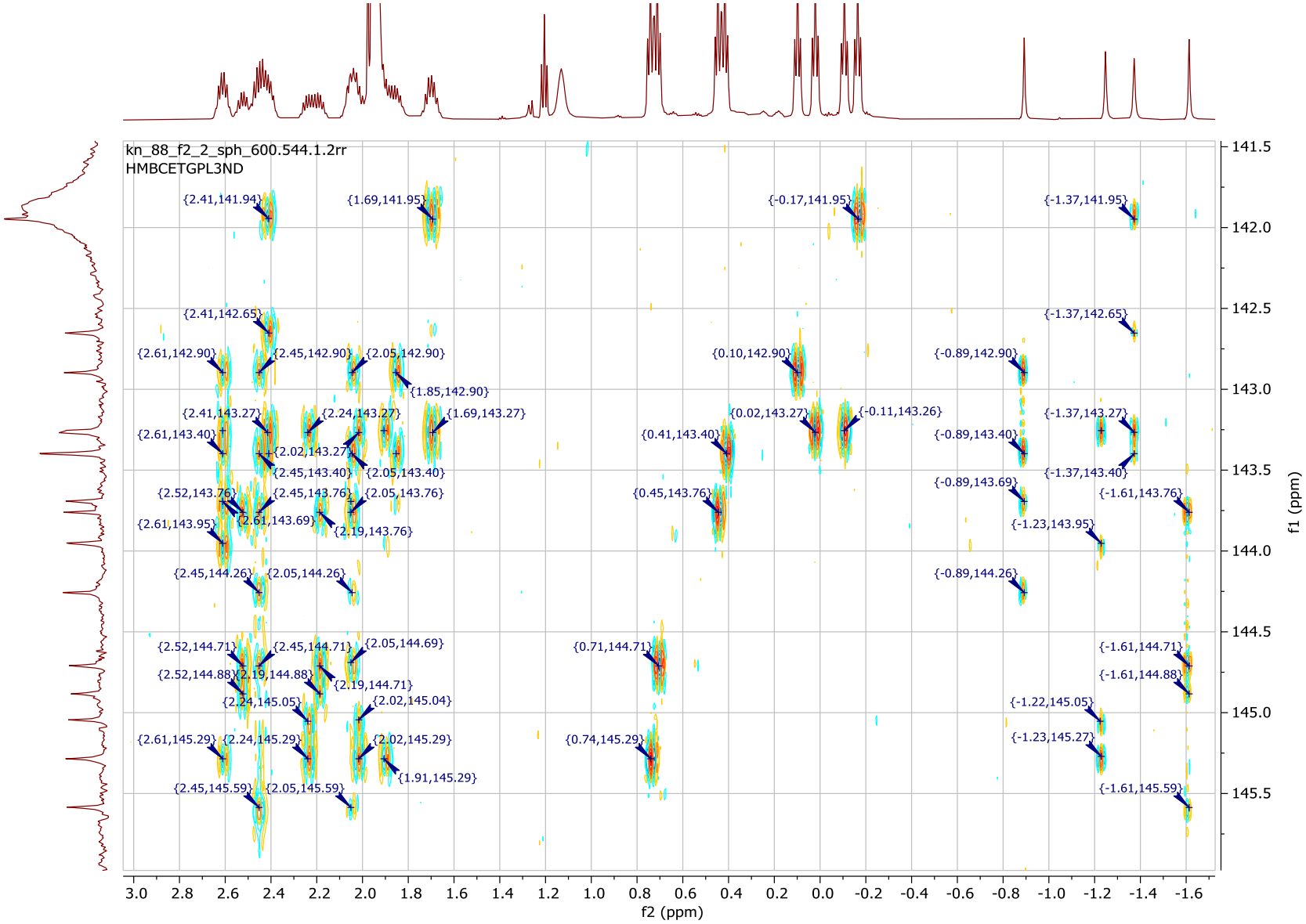

Figure S26. ^{1}H-^{13}C HMBC spectrum, expansion of area of interest of α_3,β-**P1-BSA** (acetonitrile-d_3, 25 °C).

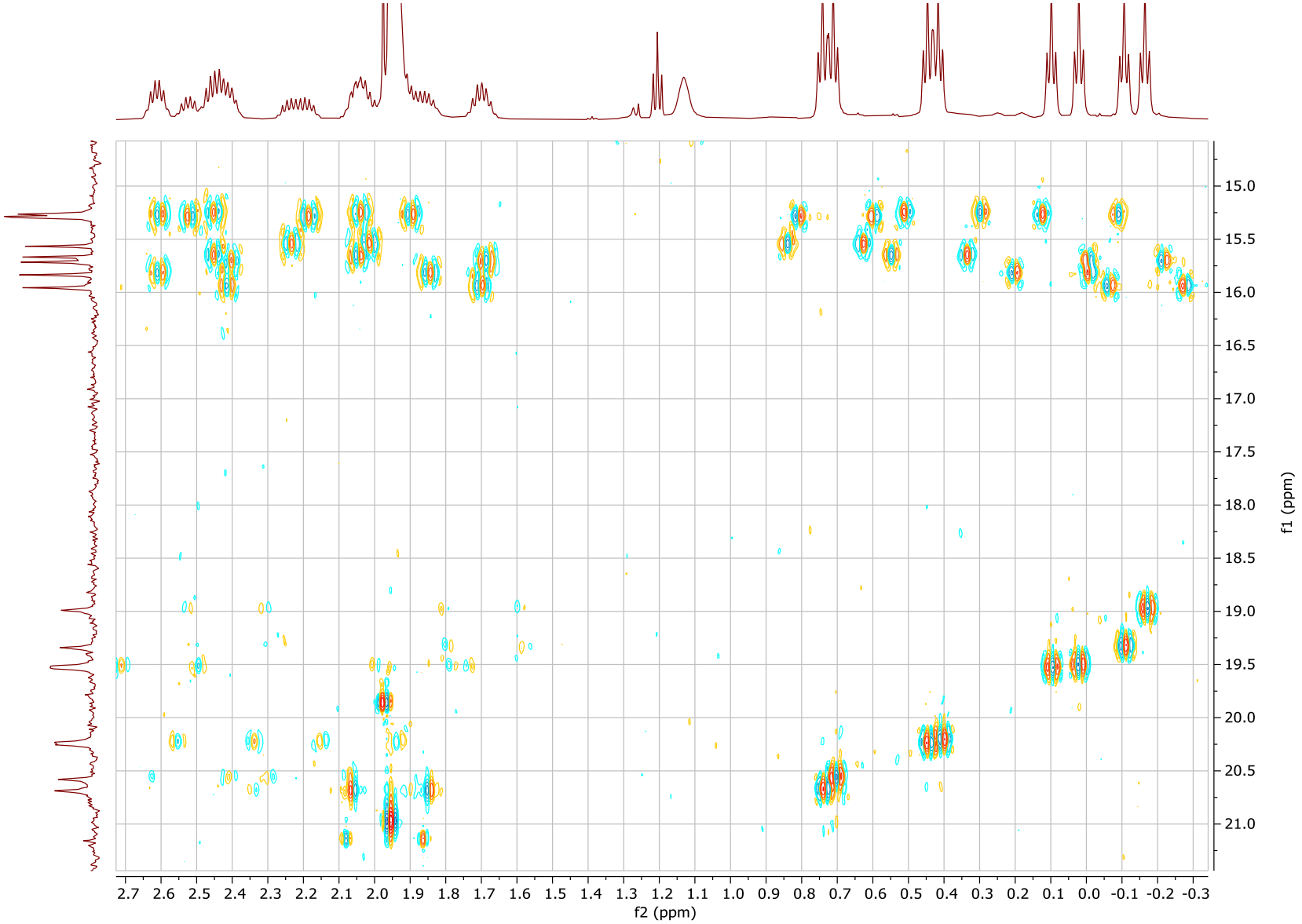

Figure S27. ^{1}H-^{13}C HMBC spectrum of $\alpha_{3,}\beta$-**P1-BSA**, expansion of aliphatic area (acetonitrile-d_3, 25 °C).

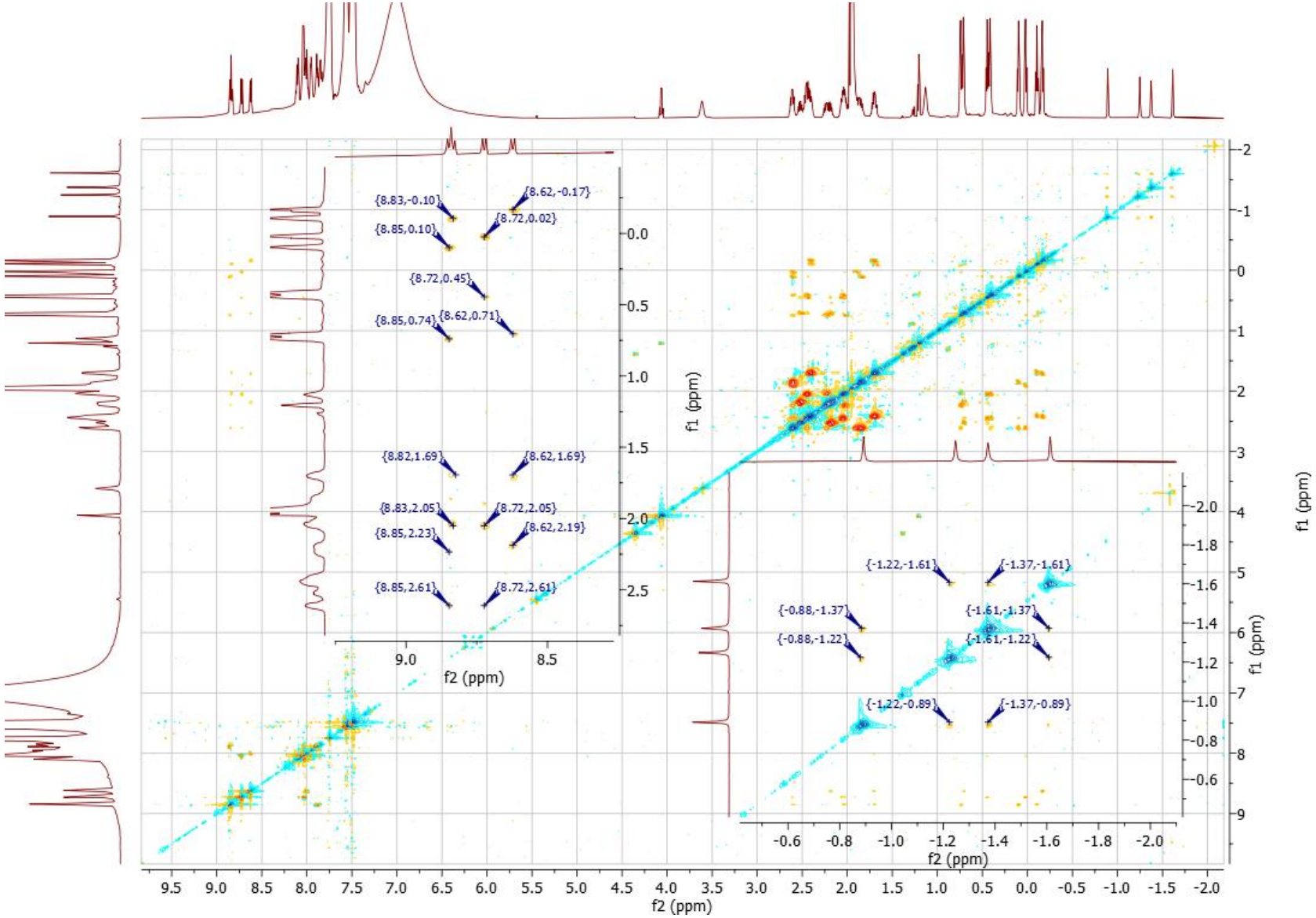

Figure S28. ^{1}H-^{1}H ROESY spectrum of $\alpha_{3,}\beta$-**P1-BSA** with expansion of areas of interest (acetonitrile-d_3, 25 °C).

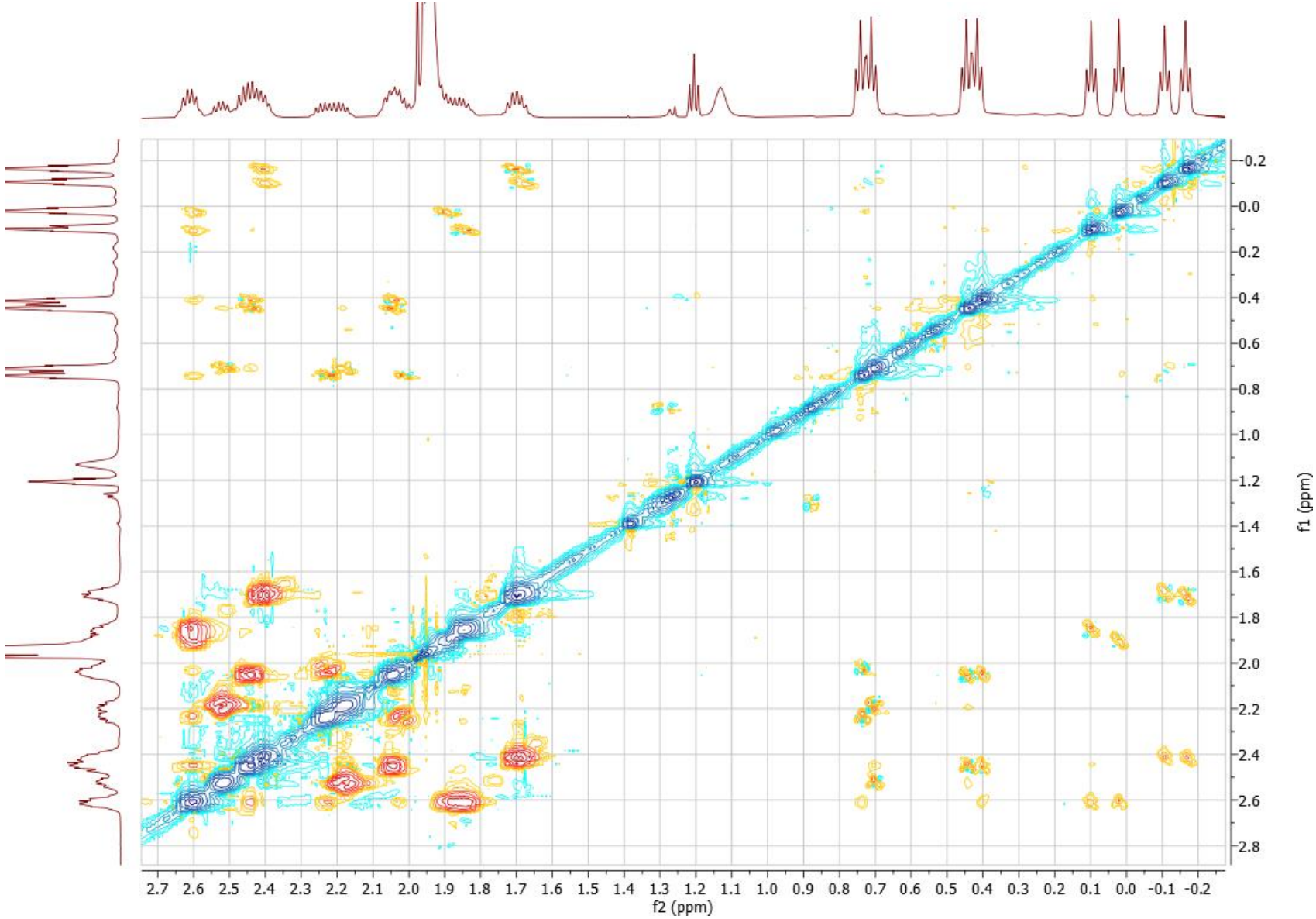

Figure S29. ^{1}H-^{1}H ROESY spectrum of $\alpha_{3,}\beta$-**P1-BSA**, expansion of aliphatic area (acetonitrile-d_3, 25 °C).

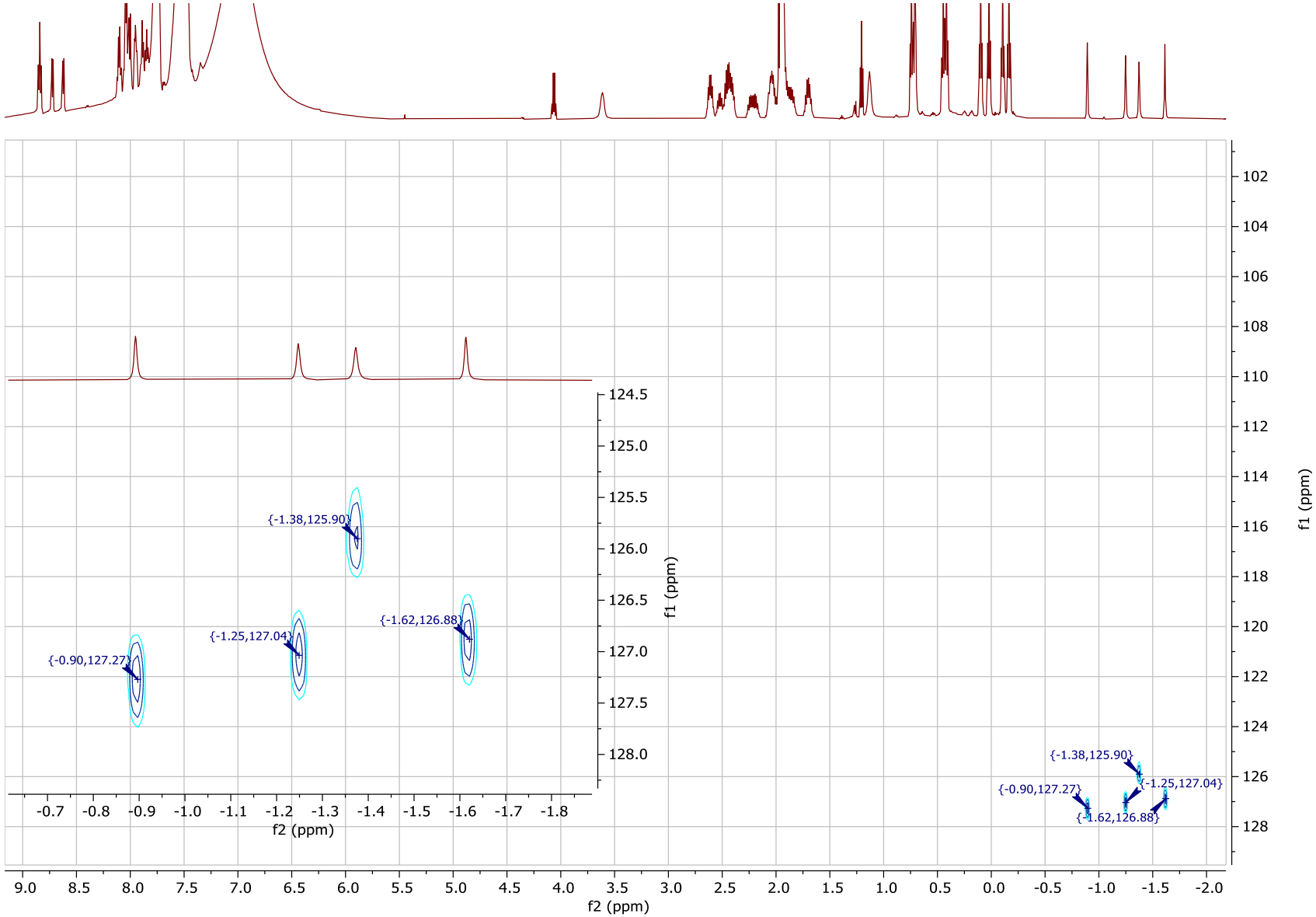

Figure S30. ^{1}H-^{15}N HSQC spectrum of $\alpha_{3,}\beta$-**P1-BSA** with expansion of areas of interest (acetonitrile-d_3, 25 °C).

SUPPORTING INFORMATION

*Synthesis and Characterization of α_4-***P1-BSA**

α,α,α,α-5,10,15,20-Tetrakis(2-aminiumphenyl)-2,3,7,8,12,13,17,18-octaethyl-porphyrin hexa-benzenesulfonic acid salt (*α_4*-P1-BSA). In a sample tube benzene sulfonic acid (0.82 mg; 0.25 mmol; 50 eq.) was dissolved in 1 mL of acetonitrile-d_3. Isomerically pure [α,α,α,α-5,10,15,20-tetrakis(2-aminophenyl)-2,3,7,8,12,13,17,18-octaethylporphyrinato]nickel(II) (5 mg; 0.005 mmol; 1 eq.) was added in one batch and stirred for 16 hours. The completion of demetalation followed by complex formation was identified by a clear color change (maroon to green) of the solution. During slow evaporation, green/blue shard habit crystals were formed. ^{1}H NMR (600 MHz, acetonitrile-d_3) δ = 8.63 (d, *J* = 7.6 Hz, 4H, Ar-*H*), 8.13 (t, *J* = 7.8 Hz, 4H, Ar-*H*), 8.04 – 7.98 (m, 8H, Ar-*H*), 2.62 (dq, *J* = 15.1, 7.5 Hz, 4H, C*H*$_2$ (b)), 2.54 (dq, *J* = 15.0, 7.5 Hz, 4H, C*H*$_2$ (a)), 2.20 (dq, *J* = 15.1, 7.6 Hz, 4H, C*H*$_2$ (b)), 1.78 (dq, *J* = 15.0, 7.5 Hz, 4H, C*H*$_2$ (a)), 0.57 (t, *J* = 7.6 Hz, 12H, C*H*$_3$ (b)), 0.08 (t, *J* = 7.5 Hz, 12H, C*H*$_3$ (a)), -0.82 (s, 2H, N-*H* (a)), -2.58 (s, 2H, N-*H* (b)) ppm.; ^{13}C NMR (151 MHz, acetonitrile-d_3) δ = 143.22 (α-pyrrole (a)), 142.19 (β-pyrrole (a)), 144.9 (α-pyrrole (b)), 144.77 (β-pyrrole (b)), 140.56 (Ar), 134.32 (Ar), 133.01 (Ar), 131.74 (Ar), 130.72 (Ar), 126.19 (Ar), 114.09 (meso-), 18.88 (CH$_2$ (a)), 20.44 (CH$_2$ (b)), 15.01 (CH$_3$ (b)), 16.15 (CH$_3$ (a)) ppm.; ^{15}N NMR (61 MHz, acetonitrile-d_3) δ 125.09 (N-H (a)), 125.80 (N-H (b)) ppm.

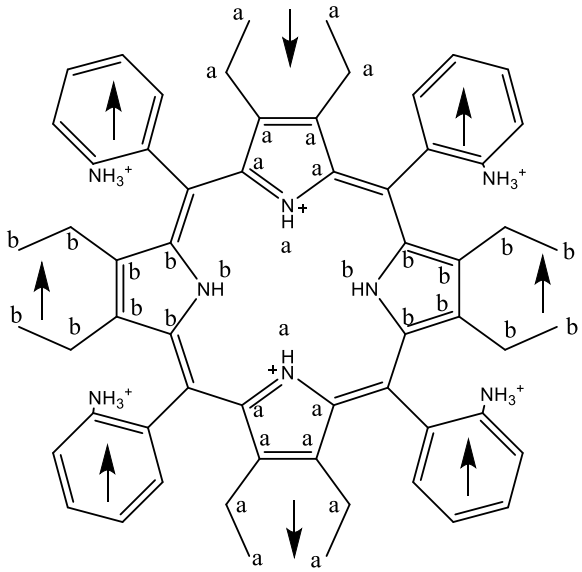

Figure S31. Structure of *α_4*-**P1-BSA** highlighting the positions used in NMR characterizations.

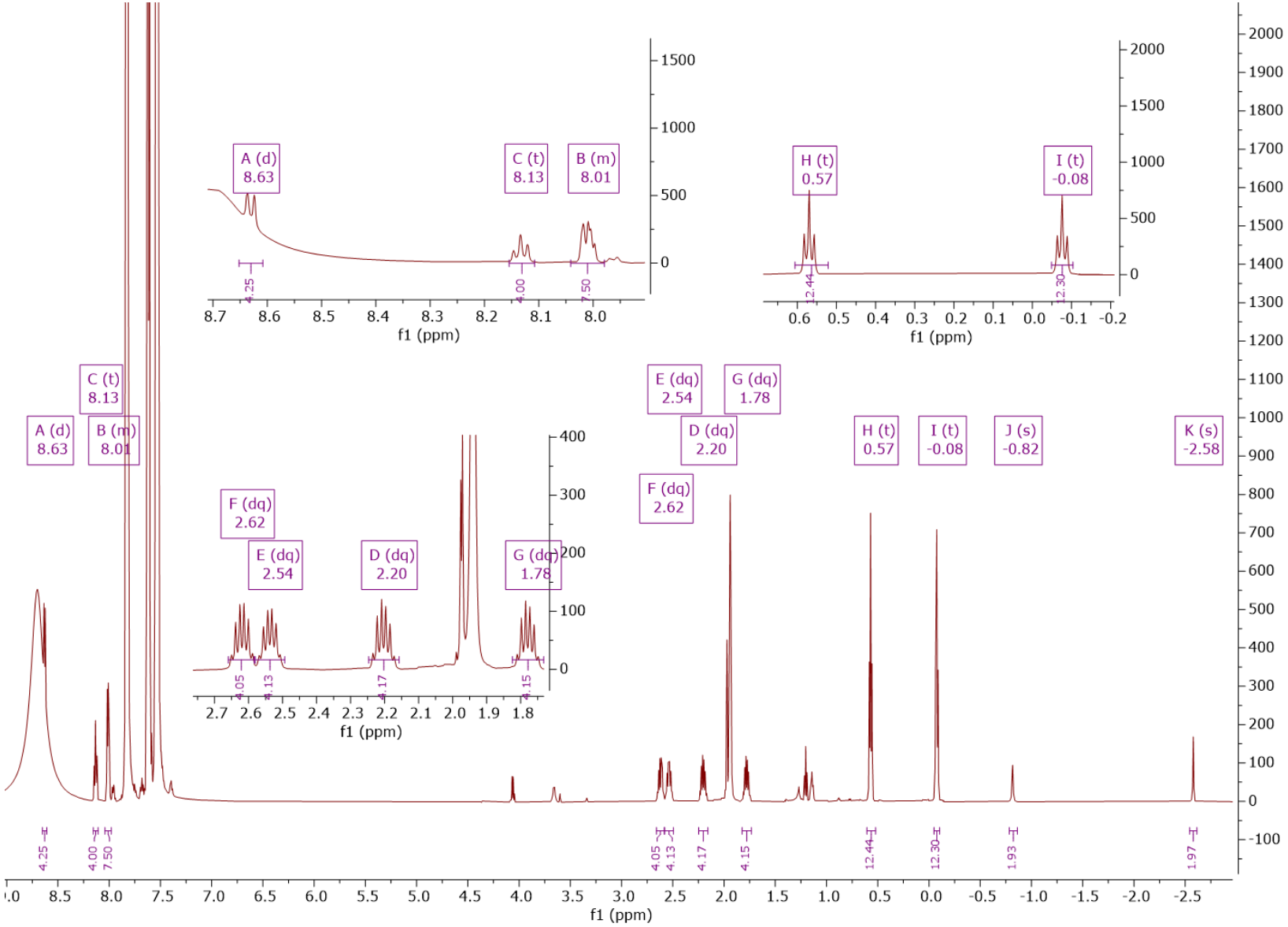

Figure S32. ^{1}H NMR spectrum of *α*$_4$-**P1-BSA** with expansion of areas of interest (600 MHz, acetonitrile-*d*$_3$, 25 °C).

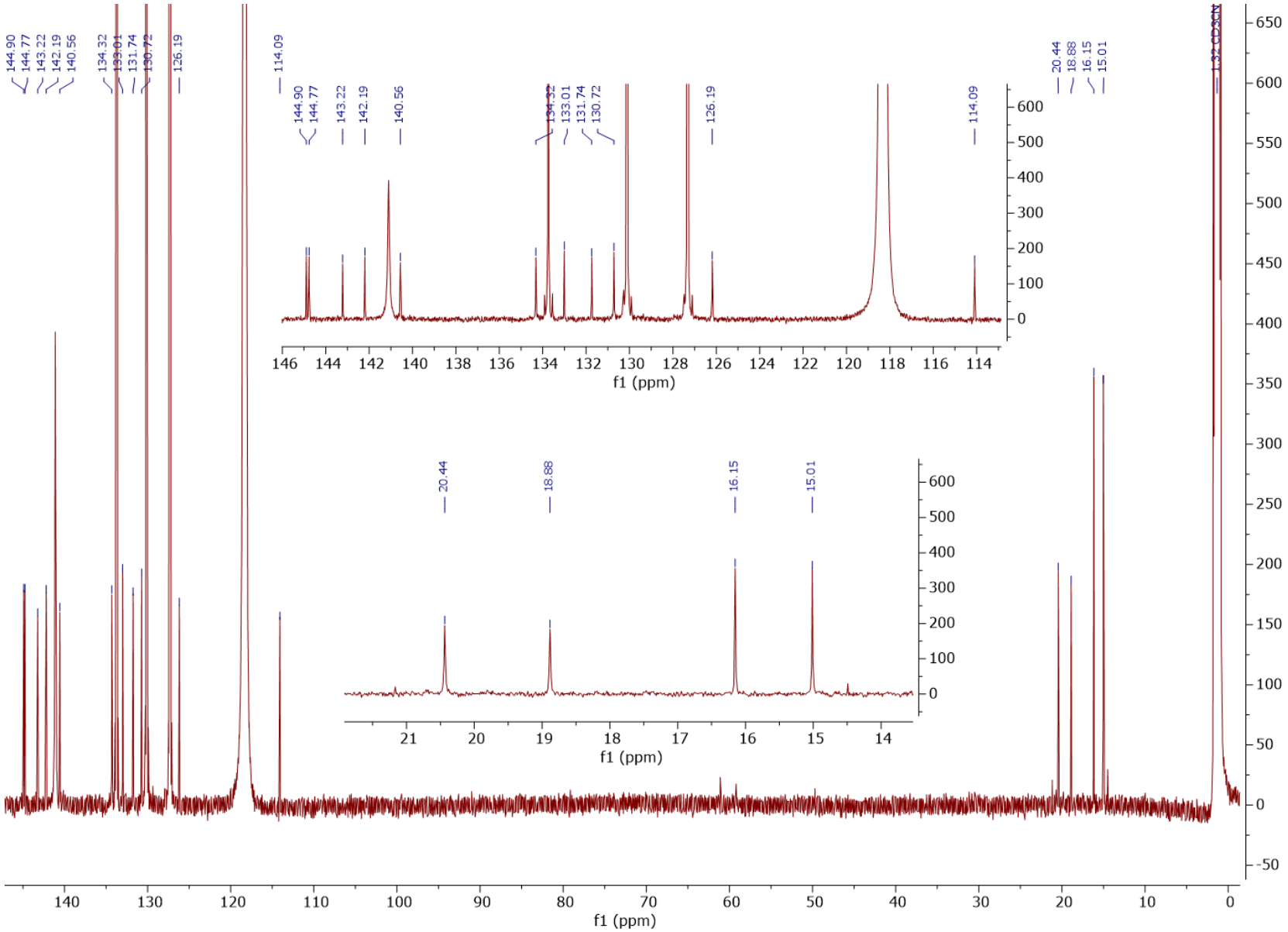

Figure S33. ^{13}C NMR spectrum of *α*$_4$-**P1-BSA** with expansion of areas of interest (151 MHz, acetonitrile-*d*$_3$, 25 °C).

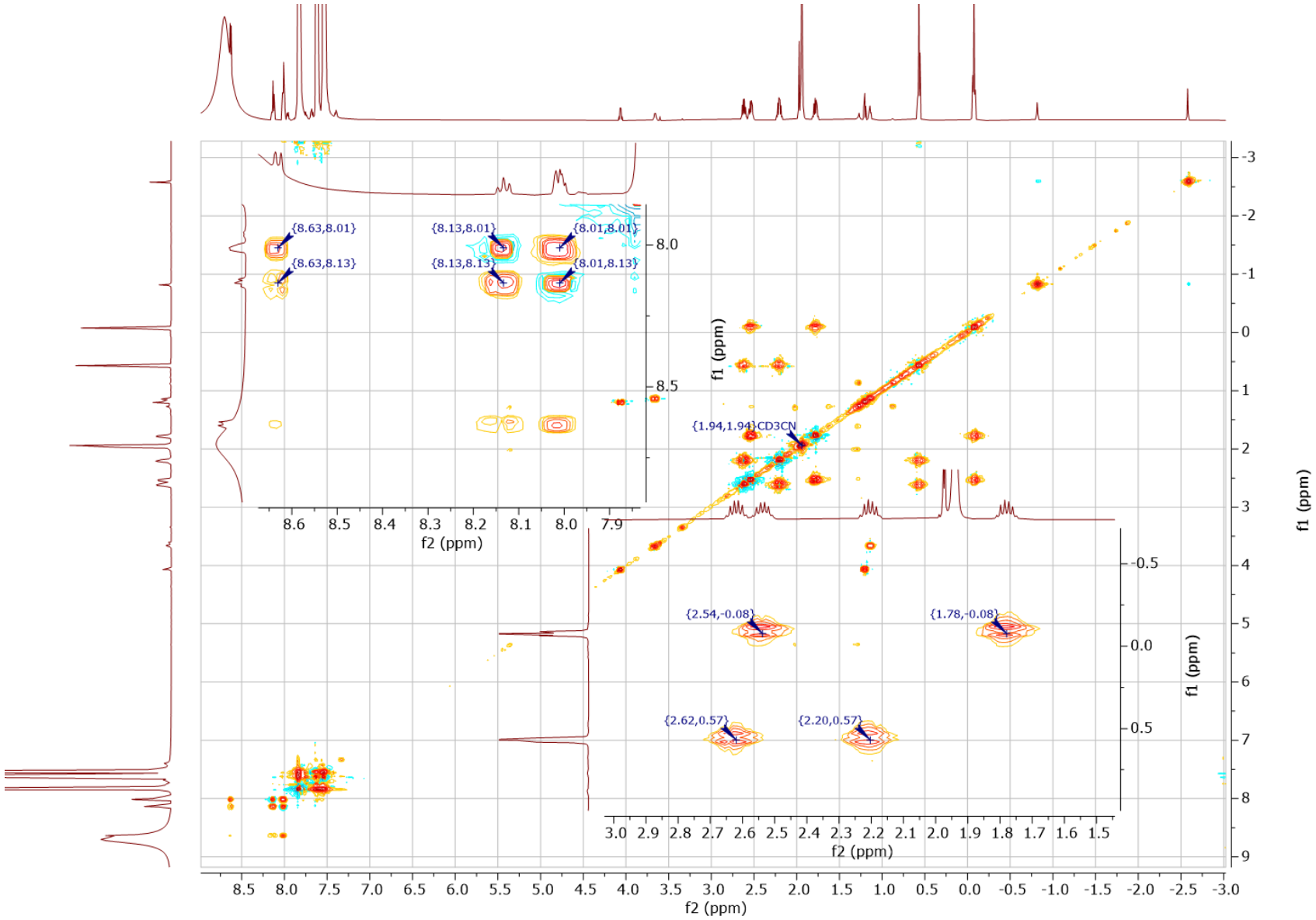

Figure S34. ^{1}H–^{1}H TOCSY spectrum of α_4-**P1-BSA** with expansion of areas of interest (acetonitrile-d_3, 25 °C).

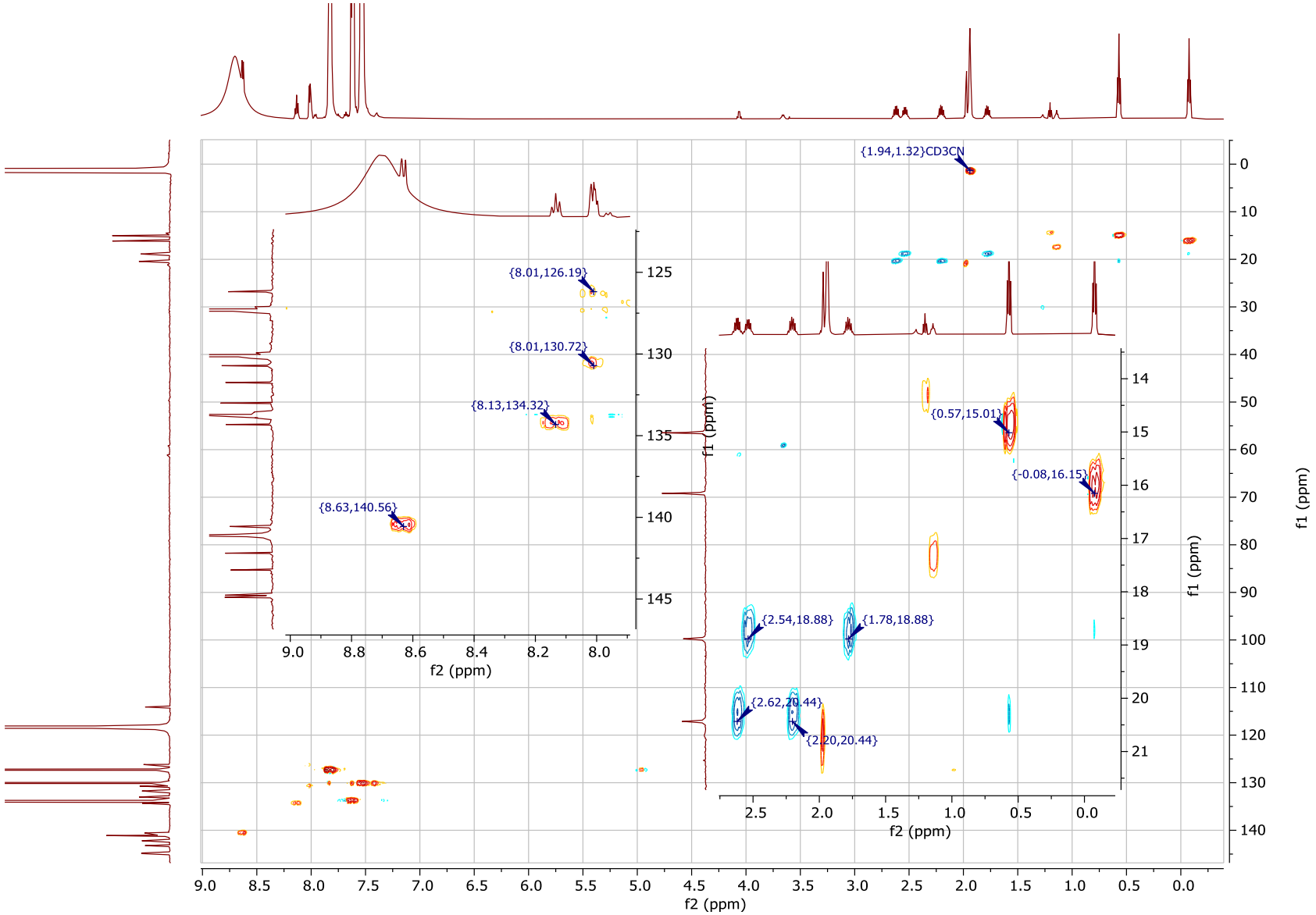

Figure S35. ^{1}H-^{13}C HSQC spectrum of *α*$_4$-**P1-BSA** with expansion of areas of interest (acetonitrile-*d*$_3$, 25 °C).

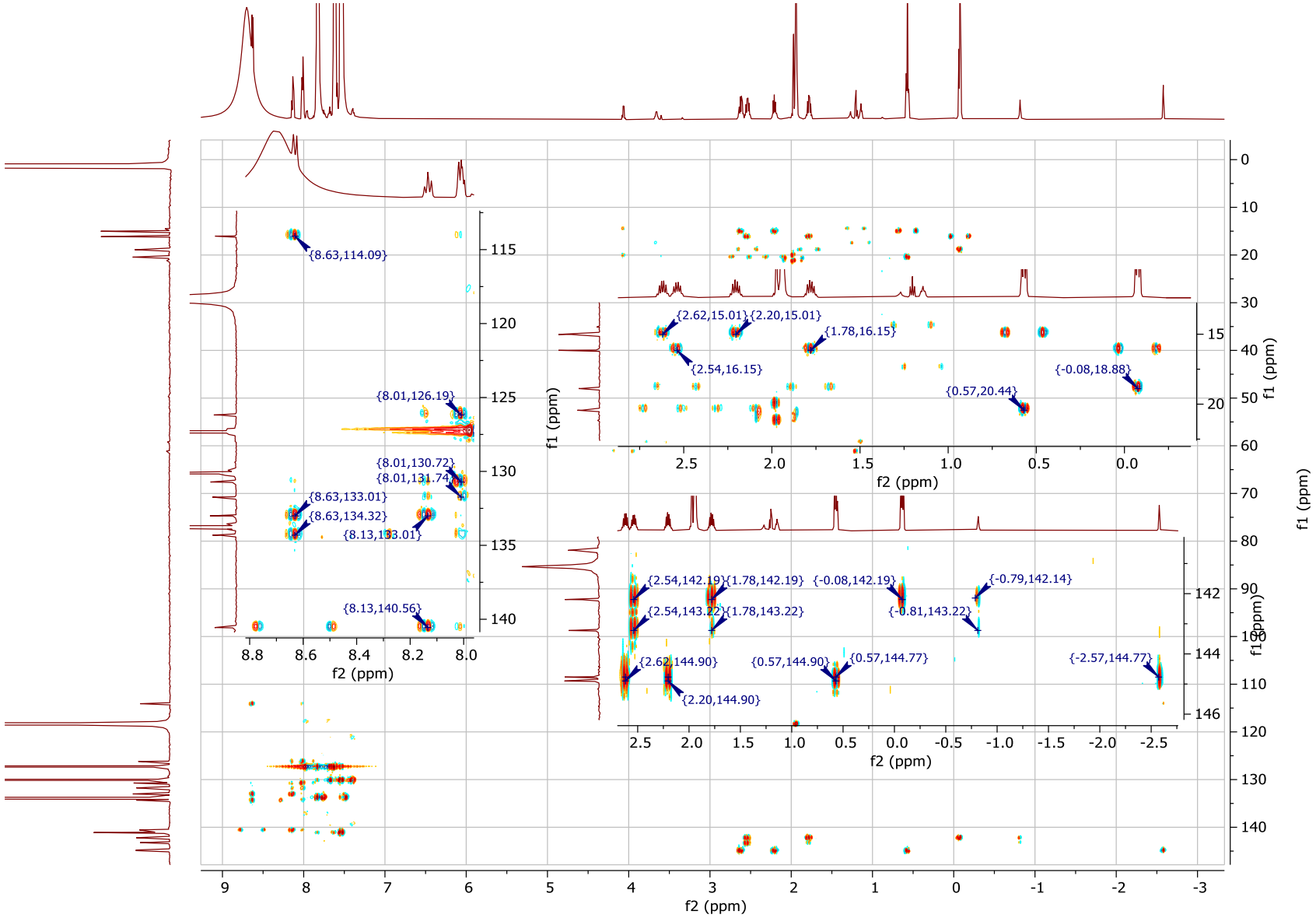

Figure S36. ^{1}H-^{13}C HMBC spectrum of α_4-**P1-BSA** with expansion of areas of interest (acetonitrile-d_3, 25 °C).

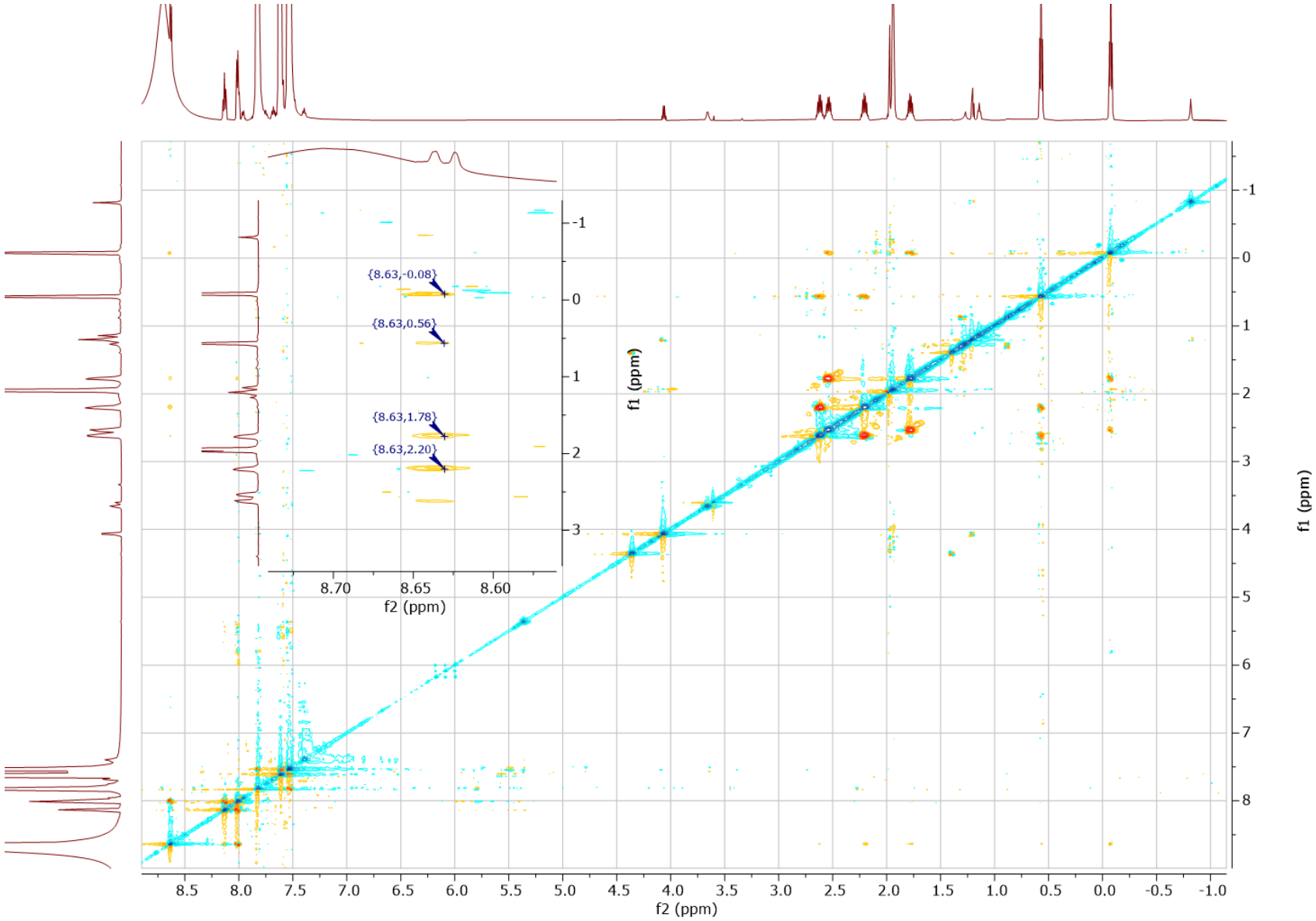

Figure S37. ^{1}H-^{1}H ROESY spectrum of α_4-**P1-BSA** with expansion of areas of interest (acetonitrile-d_3, 25 °C).

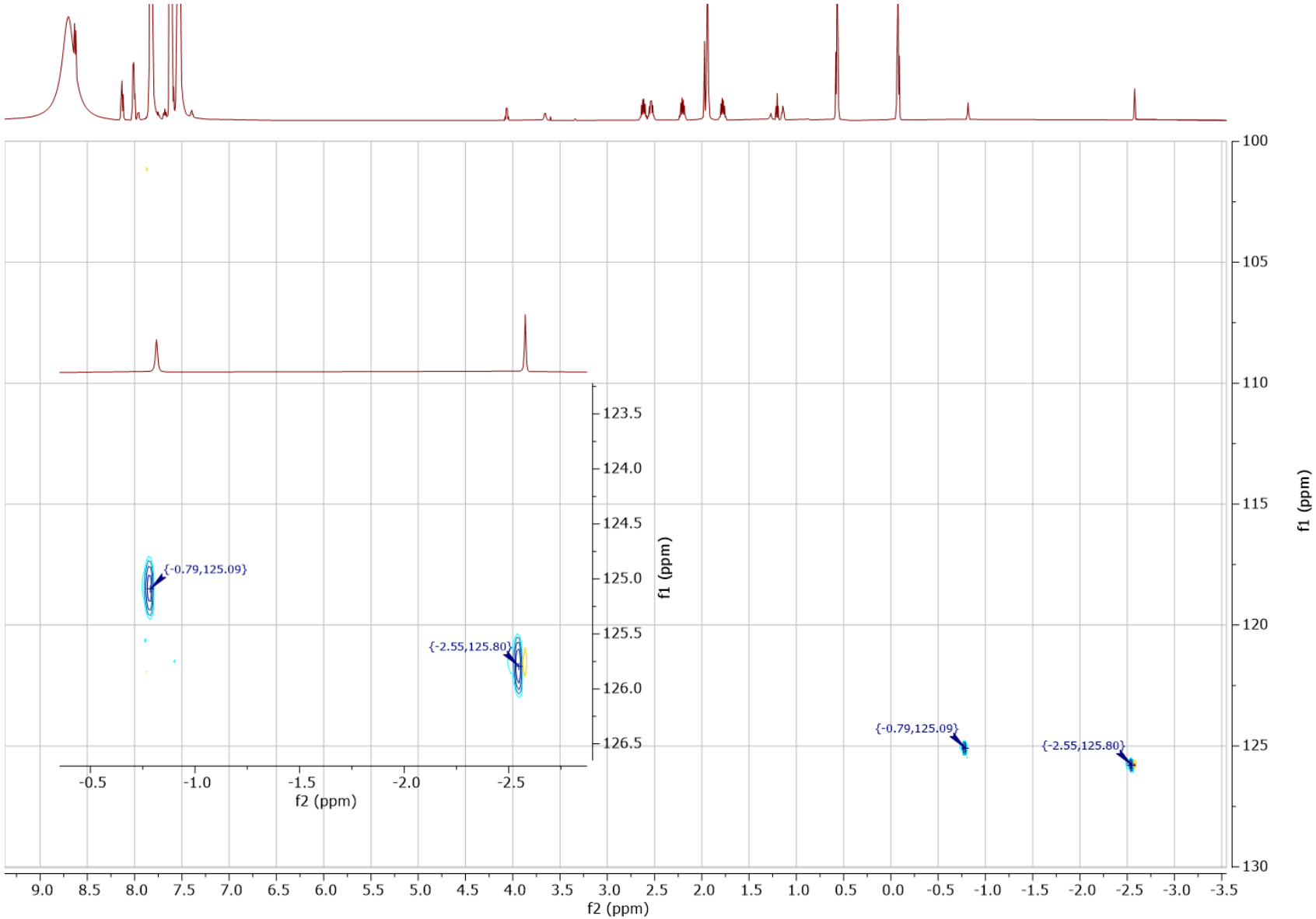

Figure S38. ^{1}H-^{15}N HSQC spectrum of α_4-**P1-BSA** with expansion of areas of interest (acetonitrile-d_3, 25 °C).

SUPPORTING INFORMATION

Determination of Atropisomeric Mixtures by NMR

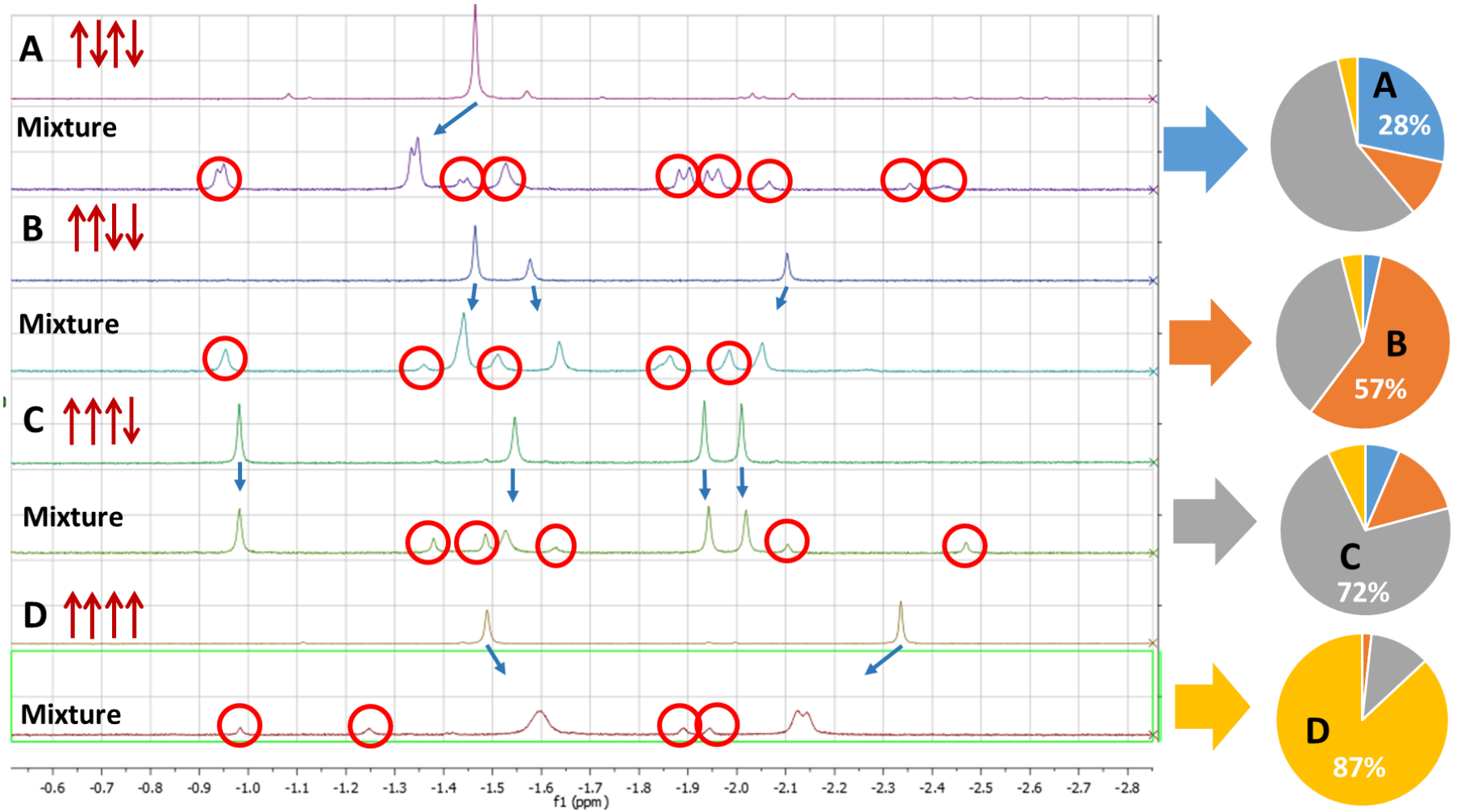

Figure S39. An example of atropisomeric mixture determination by ^{1}H NMR analysis of the porphyrin **P1-MSA** (A: $\alpha,\beta,\alpha,\beta$-; B: α_2,β_2-; C: α_3,β-; D: α_4-) inner core (N–H) signals (acetonitrile-d_3, 25 °C). The mixtures were randomly generated to create comprehensive studies of the unknown samples. The percentage values were obtained by integration of the proton signal

SUPPORTING INFORMATION

Table S1. ^{1}H, ^{13}C and ^{15}N NMR signals of **P1-BSA** atropisomers obtained from HSQC and HMBC in CD_3CN (δ in ppm). Blue – above and red – below the plane, purple – either above or below the plane depending on the orientation of $-NH_3^+$ groups.

Pos.	$\alpha_3\beta$-P1-BSA		$\alpha_2\beta_2$-P1-BSA		$\alpha,\beta,\alpha,\beta$-P1-BSA		α_4-P1-BSA	
	δ_H	δ_C or δ_N	δ_H	δ_C or δ_N	δ_H	δ_C or δ_N	δ_H	δ_C or δ_N
1		145.1		144.9		143.6		144.9
2		145.3		145.6		143.8		144.8
2^1(inner)	1.91	19.5	2.48	20.8	1.86	19.8	2.62	20.4
2^1(outer)	2.61		2.19		2.63		2.20	
2^2	0.02	15.3	0.71	15.4	0.05	15.3	0.57	15.0
3		143.3		145.6		144.0		144.8
3^1(inner)	2.02	20.7	2.48	20.8	2.38	20.6	2.62	20.4
3^1(outer)	2.24		2.19		2.06		2.20	
3^2	0.74	15.6	0.71	15.4	0.62	15.6	0.57	15.0
4		144.0		144.9		145.0		144.9
5		113.4		112.0		113.1		114.1
5^1		132.2		132.0		132.1		131.7
5^2		133.5		133.0		132.9		133.0
5^3	7.96	126.1	7.90	125.9	8.02	126.0	8.01	126.2
5^4	8.03	134.1	8.08	134.2	8.11	134.4	8.13	134.3
5^5	7.89	130.4	7.94	130.5	7.99	130.9	8.01	130.7
5^6	8.85	139.4	8.74	140.4	8.92	140.1	8.63	140.6
6		143.7		144.1		143.6		143.2
7		142.9		142.0		143.8		142.2
7^1(inner)	1.85	19.5	2.63	19.1	1.86	19.8	2.54	18.2
7^1(outer)	2.61		1.85		2.63		1.78	
7^2	0.10	15.8	–0.04	15.9	0.05	15.3	0.08	16.2
8		143.4		143.9		144.0		142.2
8^1(inner)	2.45	20.2	2.48	20.5	2.38	20.6	2.54	18.2
8^1(outer)	2.05		2.09		2.06		1.78	
8^2	0.42	15.3	0.67	15.2	0.62	15.6	0.08	16.2
9		144.3		143.9		145.0		143.2
10		114.9		114.9		113.1		114.1
10^1		131.9		132.1		132.1		131.7
10^2		133.0		133.1		132.9		133.0
10^3	7.94	125.8	8.06	126.4	8.02	126.0	8.01	126.2
10^4	8.04	134.1	8.12	134.2	8.11	134.4	8.13	134.3
10^5	7.85	130.6	8.03	130.6	7.99	130.9	8.01	130.7
10^6	8.83	140.8	8.66	139.8	8.92	140.1	8.63	140.6
11		143.4		142.8		143.6		144.9
12		143.3		142.9		143.8		144.8
12^1(inner)	2.41	19.3	2.37	19.1	1.86	19.8	2.62	20.4
12^1(outer)	1.69		1.66		2.63		2.20	
12^2	–0.11	15.7	–0.19	15.9	0.05	15.3	0.57	15.0
13		142.0		142.9		144.0		144.8
13^1(inner)	2.41	19.0	2.37	19.1	2.38	20.6	2.62	20.4
13^1(outer)	1.71		1.66		2.06		2.20	
13^2	–0.16	16.0	–0.19	15.9	0.62	15.6	0.57	15.0
14		142.7		142.8		145.0		144.9
15		113.4		114.9		113.1		114.1
15^1		132.2		132.1		132.1		131.7
15^2		133.1		133.1		132.9		133.0
15^3	8.00	126.1	8.06	126.4	8.02	126.0	8.01	126.2
15^4	8.11	134.2	8.12	134.2	8.11	134.4	8.13	134.3
15^5	8.00	130.5	8.03	130.6	7.99	130.9	8.01	130.7
15^6	8.62	140.4	8.66	139.8	8.92	140.1	8.63	140.6
16		145.6		143.9		143.6		143.2
17		143.8		143.9		143.8		142.2
17^1(inner)	2.52	20.6	2.48	20.5	1.86	19.8	2.54	18.2
17^1(outer)	2.19		2.09		2.63		1.78	
17^2	0.71	15.3	0.67	15.2	0.05	15.3	0.08	16.2
18		144.7		142.0		144.0		142.2
18^1(inner)	2.45	20.2	2.63	19.1	2.38	20.6	2.54	18.2
18^1(outer)	2.05		1.85		2.06		1.78	
18^2	0.45	15.7	–0.04	15.9	0.62	15.6	0.08	16.2
19		144.9		144.1		145.0		143.2
20		111.5		112.0		113.1		114.1
20^1		131.9		132.0		132.1		131.7
20^2		133.2		133.0		132.9		133.0
20^3	8.04	126.1	7.90	125.9	8.02	126.0	8.01	126.2
20^4	8.09	134.1	8.08	134.2	8.11	134.4	8.13	134.3
20^5	8.03	130.7	7.94	130.5	7.99	130.9	8.01	130.7
20^6	8.72	140.2	8.74	140.4	8.92	140.1	8.63	140.6
21	–1.25	127.0	–2.15	125.9	–1.42	126.5	–2.58	125.8
22	–0.89	127.3	–1.08	127.0	–1.42	126.5	–0.82	125.1
23	–1.37	125.9	–1.38	126.9	–1.42	126.5	–2.58	125.8
24	–1.61	126.9	–1.08	127.0	–1.42	126.5	–0.82	125.1

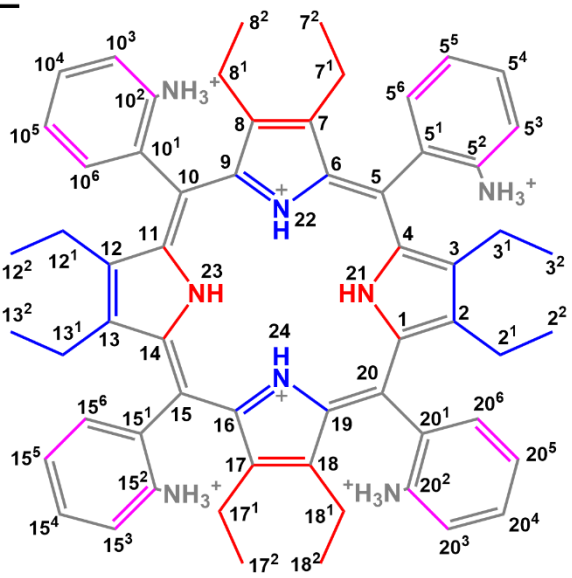

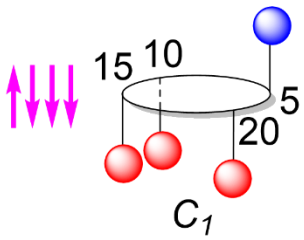

C_1

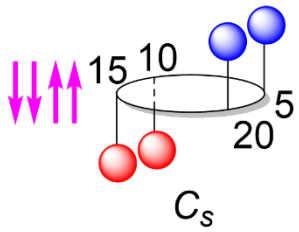

C_s

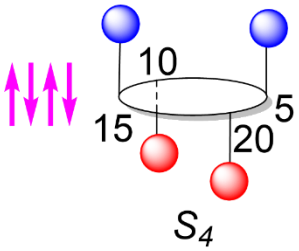

S_4

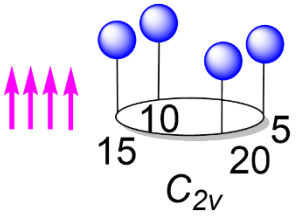

C_{2v}

SUPPORTING INFORMATION

Structural Determination of Receptor-Substrate Complexes and Atropisomers

In the structure of *α*$_{3}$,*β*-**P1**•[HSO_4^-]$_6$[H_2SO_4][CH_3OH][H_2O]$_4$ the counter anion HSO_4^- was modeled over two positions S3, S1D using rigid models and SIMU, SADI, ISOR restraints in an 80:20 % occupancy. Another HSO_4^- entity was modeled over three positions (S4, S1D, S1C) using rigid models and SIMU restraint in a 50:30:20 % occupancy. Yet another HSO_4^- was modeled over four positions (S2D, S2C, S2B, S5) using rigid models and SIMU restraint in a 20:10:20:50 % occupancy. One H_2SO_4 was modeled over three positions (S7, S3D, S1A) using rigid models and SIMU restraint in a 30:30:40 % occupancy. One MeOH molecule was modeled over four positions (C2S, C1S, C3S, C4S) using SIMU, ISOR, SADI and DFIX restraint in a 25:25:20:30 % occupancy. One of the solvent H_2O molecules was modeled over two positions (O2CA and O32) using restraint ISOR in a 40:60 % occupancy. All of the phenyl rings of the porphyrin at C5, C10, C15, and C20 were modeled over two positions at 43:57, 50:50, 74:26, 50:50 and fixed using command AFIX 66, SIMU and SADI. Six of the ethyl groups at C2, C3, C8, C12, C13, and C17 were modeled over two positions at 10:90, 24:74, 62:38, 49:51, 26:74 and 10:90 % occupancy, respectively using SIMU and SADI restraints.

In the structure of *α*$_{4}$-**P1**•[$C_6H_5SO_3^-$]$_6$[H_2O][CD_3CN]$_2$ two of the acetonitrile solvent molecules were modeled over seven positions (N5, N6, N7, N4A, N3A, N1A, N2A) using rigid models and SIMU restrains in 15:50:50:25:20:25:15 % occupancy. One of the benzenesulfonic acids was modeled over two positions (S1B, S3) using rigid models and SIMU, DFIX restraints in a 55:45 % occupancy. Phenyl rings of three benzenesulfonic acids were modeled over two positions (S1, S2, S5) using AFIX 66, SIMU and DFIX restraints in a 40:60 %, 67:33 %, 75:25 % occupancy, respectively. Moreover, benzenesulfonic acid (S5) oxygen atoms were modeled in 75:25 % occupancy along with the phenyl ring. Three ethyl groups at C7, C8, and C13 were modeled over two positions in 71:29 %, 17:29 %, 55:45 % occupancy, respectively using SIMU and SADI restrains.

In the structure of *α*$_{3}$,*β*-**P1**•[$C_6H_5SO_3^-$]$_6$[H_2O]$_2$ three of the benzenesulfonic acid molecules were modeled over 2 positions (S3 and S1A, S5 and S3A, S1 and S1C) using rigid models and SIMU restrains in 53:47%, 36:64% 60:40% occupancy, respectively. Oxygen atoms of two benzenesulfonic acid molecules (S2 and S4) were modeled over 2 positions using SIMU and SADI restrains in 75:25 %, 26:74 % occupancy, respectively. One of the benzenesulfonic acid molecule was modeled over 5 positions (S1D, S1B, S2A, S2C, and S6) using rigid models and SIMU restraints in 20:25:15:25:15 % occupancy. The ethyl group at C13 was modeled over 2 positions in 24:76 % occupancy using SIMU and SADI restraints. Another ethyl group was modeled over two positions (C1A and C2) in 72:28 % occupancy using SIMU and SADI restraints. One of the phenyl rings at C20 was modeled over two positions in 40:60 % occupancy and fixed using command AFIX 66, SIMU and SADI. The structure contains a solvent accessible void that contained a small number of solvent molecules (around 38 electrons), possibly methanol or acetonitrile; however, due to high disorder, these could not be modeled and were omitted using PLATON squeeze.

In the structure of *α*$_{4}$-**1**•[$(CH_3)_2SO$]$_5$ three of the dimethyl sulfoxide molecules were modeled over 2 positions (S1 and S1A, S4 and S4A, S3 and S3A, S5 and S5A) using SIMU and SUMP restraints in 4:96%, 89:11% 93:7% occupancies, respectively. One of the dimethyl sulfoxide solvent molecules was modeled over 3 positions (S8, S8A, and S5B) using SIMU and SUMP restraints in 56:27:17 % occupancy.

In the structure of **CP1**•[BF_4^-]$_2$ the collected diffraction pattern was found to have cubic symmetry, and a solution was found in cubic space group $I\bar{4}$ 3d. This compound was disordered over two orientations related by 180-degree rotation of the aryl rings in a refined ratio of 0.50(11) : 0.50(11). One of the ethyl groups was similarly disordered over two positions, between a pseudo-cis and pseudo-trans orientation at a refined ratio of 0.684(15) : 0.316(15). The BF_4^- anion was disordered over two overlapping symmetry-equivalent orientations and held to an occupancy of 0.5. In each case, symmetry-related atoms were held to SADI and SIMU restraints to prevent overfitting. A global loose SIMU restraint was also applied, due to weak high angle data. Due to these disordered components, the derived Flack parameter is meaningless, and no direct evidence can be brought to bear on the atropisomeric ratios in this crystal determination. The squeeze routine in PLATON was used to account for highly disordered solvent (6 water molecules per unit formula).

In the structure of *α*$_{3}$,*β*-**1** the ethyl groups at C2, C3, C7, C8, C12, C13, and C17 were modeled over 2 positions in 68:22 13:87 26:74 30:70 66:34 80:20 3:97 % occupancy, respectively using SIMU and SADI restraints. Four of the phenyl rings at C5, C10, C15, and C20 were modeled over two positions in 35:65 % occupancy and fixed using command AFIX 66, SIMU and SADI. The structure contained a solvent-accessible void with a small number of solvent molecules, possibly methanol and water or dichloromethane; however, due to a high degree of disorder, these could not be modeled and were omitted using PLATON squeeze.

SUPPORTING INFORMATION

Table S2. Details of XRD data refinement of α_4-**P1**•$[C_6H_5SO_3^-]_6[H_2O][CD_3CN]_2$, α_4-**1**•$[(CH_3)_2SO]_5$ and **CP1**•$[BF_4^-]_2$.

Compound	α_4-**P1**•$[C_6H_5SO_3^-]_6[H_2O][CD_3CN]_2$	α_4-**1**•$[(CH_3)_2SO]_5$	**CP1**•$[BF_4^-]_2$
CCDC #	2012196	2012199	2012200
Empirical formula	$C_{100}H_{104}D_6N_{10}O_{19}S_6$	$C_{70}H_{96}N_8O_5S_5$	$C_{60}H_{68}B_2F_8N_8$
Formula weight	1954.73	1289.76	1074.84
Temperature/K	100(2)	100(2)	100(2)
Crystal system	monoclinic	orthorhombic	cubic
Space group	$P2_1/n$	Pbca	$I\bar{4}$ 3d
a/Å	14.3842(4)	21.2713(8)	26.404(3)
b/Å	30.2287(10)	23.8513(8)	26.404(3)
c/Å	25.0716(8)	27.7727(9)	26.404(3)
α/°	90	90	90
β/°	104.894(2)	90	90
γ/°	90	90	90
Volume/Å^3	10535.3(6)	14090.4(8)	18409(6)
Z	4	8	12
D_{calc} g/cm^3	1.232	1.216	1.163
μ/mm^{-1}	1.761	0.218	0.086
F(000)	4113.0	5536.0	6792.0
Crystal size/mm^3	0.4 × 0.25 × 0.09	0.27 × 0.2 × 0.17	0.36 × 0.34 × 0.17
Radiation	CuKα	MoKα	MoKα
Wavelength/Å	1.54178	0.71073	0.71073
2θ/°	6.466 to 139.982	4.824 to 55.244	3.778 to 50.808
Reflections collected	97515	209918	209989
Independent reflections	19804	16280	2828
R_{int}	0.0813	0.1187	0.0559
R_{sigma}	0.0992	0.0477	0.0122
Restraints	1142	595	678
Parameters	1631	987	249
GooF	1.036	1.033	1.095
R_1 [I> 2σ (I)]	0.0924	0.0796	0.0822
wR_2 [I> 2σ (I)]	0.2748	0.1976	0.2286
R_1 [all data]	0.1253	0.1340	0.0876
wR_2 [all data]	0.3087	0.2452	0.2377
Largest peak/e Å^{-3}	1.32	1.02	0.35
Deepest hole/e Å^{-3}	-0.77	-0.82	-0.41

SUPPORTING INFORMATION

Table S3. Details of XRD data refinement of *α*$_{3}$,*β*-***1***, *α*$_{3}$,*β*-**P1**•[$C_6H_5SO_3^-$]$_6$[H_2O]$_2$ and *α*$_{3}$,*β*-**P1**•[HSO_4^-]$_6$[H_2SO_4][CH_3OH][H_2O]$_4$.

Compound	*α*$_{3}$,*β*-***1***	*α*$_{3}$,*β*-**P1**•[$C_6H_5SO_3^-$]$_6$[H_2O]$_2$	*α*$_{3}$,*β*-**P1**•[HSO_4^-]$_6$[H_2SO_4][CH_3OH][H_2O]$_4$
CCDC #	2012198	2012197	2012195
Empirical formula	$C_{60}H_{66}N_8$	$C_{96}H_{106}N_8O_{20}S_6$	$C_{61}H_{92}N_8O_{33}S_7$
Formula weight	899.20	1884.24	1689.84
Temperature/K	100(2)	100(2)	100(2)
Crystal system	triclinic	triclinic	triclinic
Space group	$P\bar{1}$	$P\bar{1}$	$P\bar{1}$
a/Å	13.4646(9)	13.890(3)	13.2007(5)
b/Å	13.7785(9)	16.457(3)	14.5421(5)
c/Å	16.0771(11)	21.147(3)	23.9326(9)
α/°	105.194(2)	81.292(5)	105.4300(10)
β/°	96.975(2)	82.916(4)	90.996(2)
γ/°	107.247(2)	80.393(6)	115.7820(10)
Volume/Å^3	2684.0(3)	4687.5(14)	3940.6(3)
Z	2	2	2
D$_{calc}$ g/cm^3	1.113	1.335	1.424
μ/mm^{-1}	0.066	1.962	0.290
F(000)	964.0	1988.0	1780.0
Crystal size/mm^3	0.34 × 0.09 × 0.06	0.25 × 0.2 × 0.1	0.455 × 0.142 × 0.056
Radiation	MoKα	CuKα	MoKα
Wavelength/Å	0.71073	1.54178	0.71073
2θ/°	5.134 to 51.088	4.248 to 139.05	5.332 to 50.5
Reflections collected	50635	43476	36013
Independent reflections	9967	17189	14224
R$_{int}$	0.1530	0.0339	0.0522
R$_{sigma}$	0.1063	0.0474	0.0760
Restraints	1034	2216	2373
Parameters	925	1819	1653
GooF	1.005	1.234	1.023
R$_1$ [I> 2σ (I)]	0.0783	0.0971	0.0942
wR$_2$ [I> 2σ (I)]	0.1868	0.2940	0.2657
R$_1$ [all data]	0.1759	0.1196	0.1457
wR$_2$ [all data]	0.2422	0.3205	0.3088
Largest peak/e Å^{-3}	0.38	0.88	1.10
Deepest hole/e Å^{-3}	-0.25	-0.78	-0.90

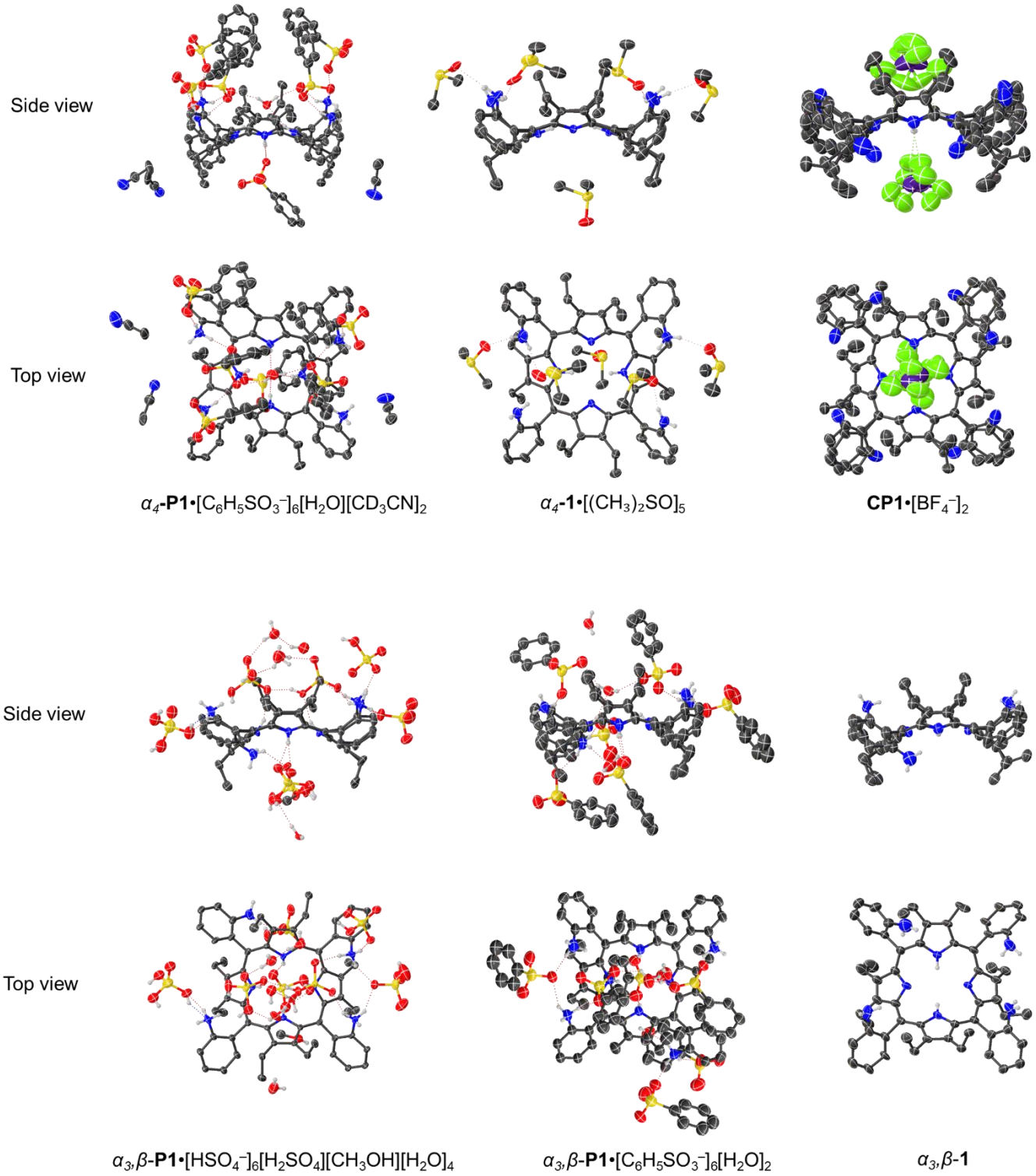

Figure S40. Side and top views of the single porphyrin units in the single crystal X-ray structures obtained. Non-essential hydrogen atoms were omitted for clarity and thermal ellipsoids give 50% probability.

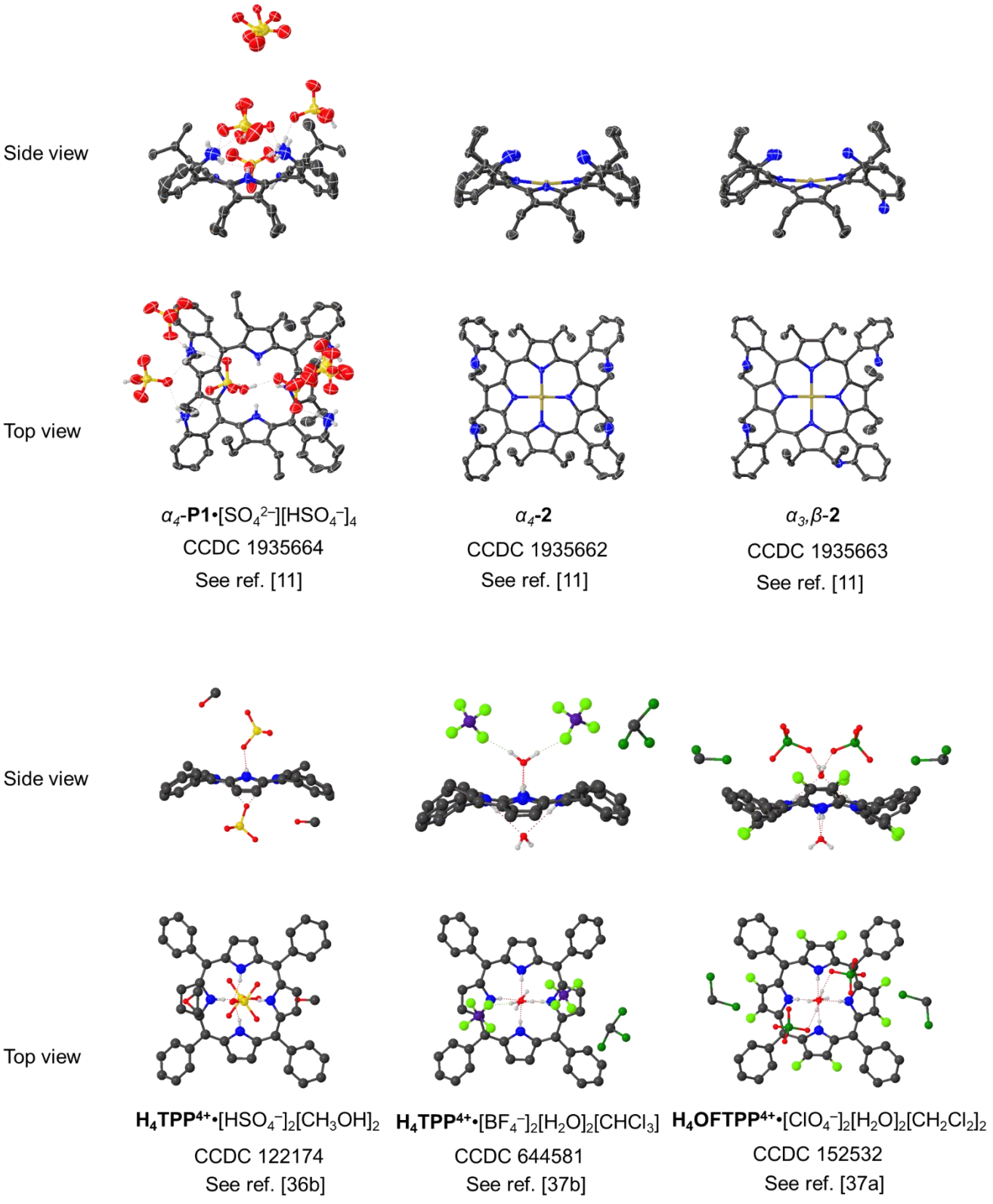

Figure S41. Side and top views of the single porphyrin units discussed. Non-essential hydrogen atoms were omitted for clarity and thermal ellipsoids give 50% probability.

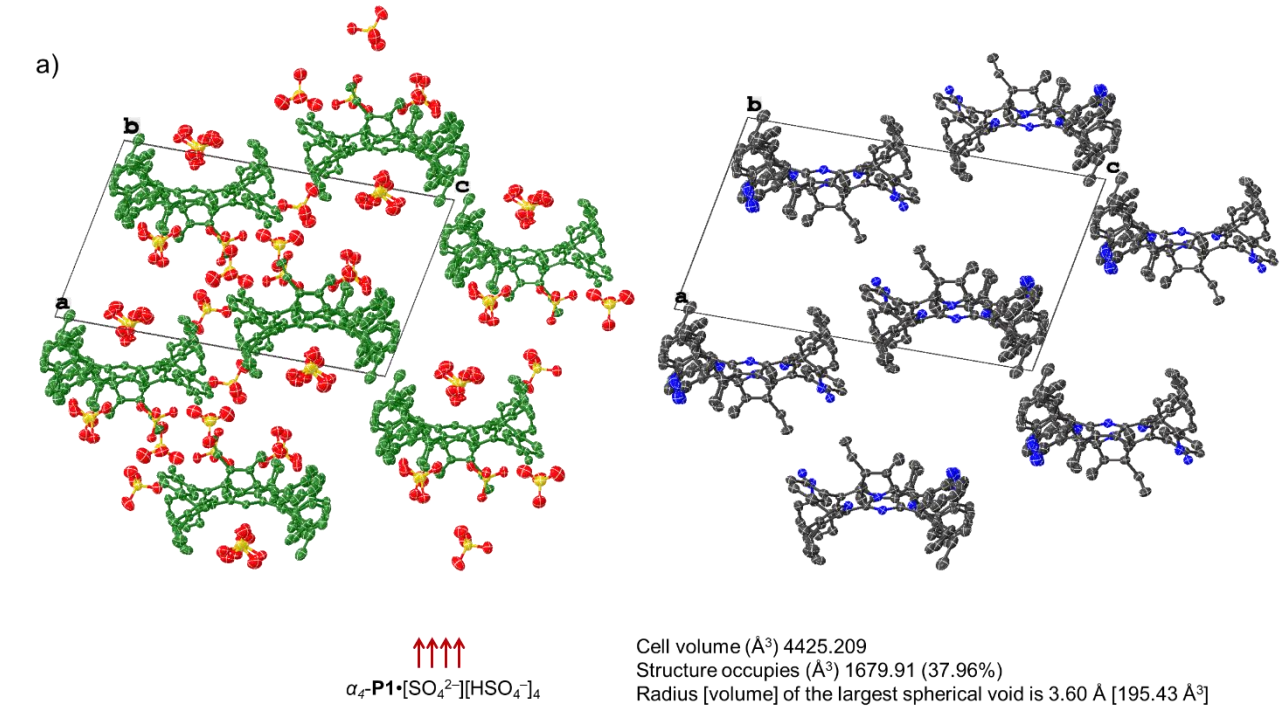

α_4-**P1**•[SO_4^{2-}][HSO_4^-]$_4$

Cell volume (Å^3) 4425.209
Structure occupies (Å^3) 1679.91 (37.96%)
Radius [volume] of the largest spherical void is 3.60 Å [195.43 Å^3]

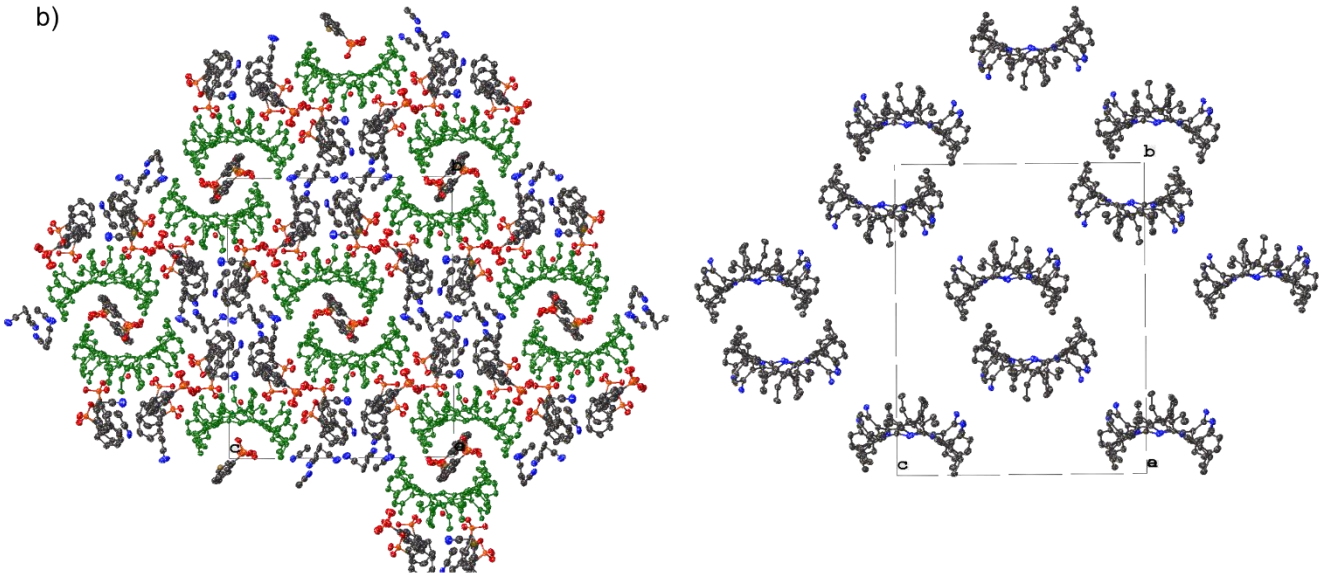

α_4-**P1**•[$C_6H_5SO_3^-$]$_6$[H_2O][CD_3CN]$_2$

Cell volume (Å^3) 10535.266
Structure occupies (Å^3) 3303.21 (31.35%)
Radius [volume] of the largest spherical void is 4.80 Å [463.25 Å^3]

Figure S42. Crystal packing illustrations of a) α_4-**P1**•[SO_4^{2-}][HSO_4^-]$_4$ and b) α_4-**P1**•[$C_6H_5SO_3^-$]$_6$[H_2O][CD_3CN]$_2$. On the left, single units are highlighted in green; on the right, representation of single units without counter anions and solvents (non-essential hydrogen atoms omitted for clarity and thermal ellipsoids give 50% probability).

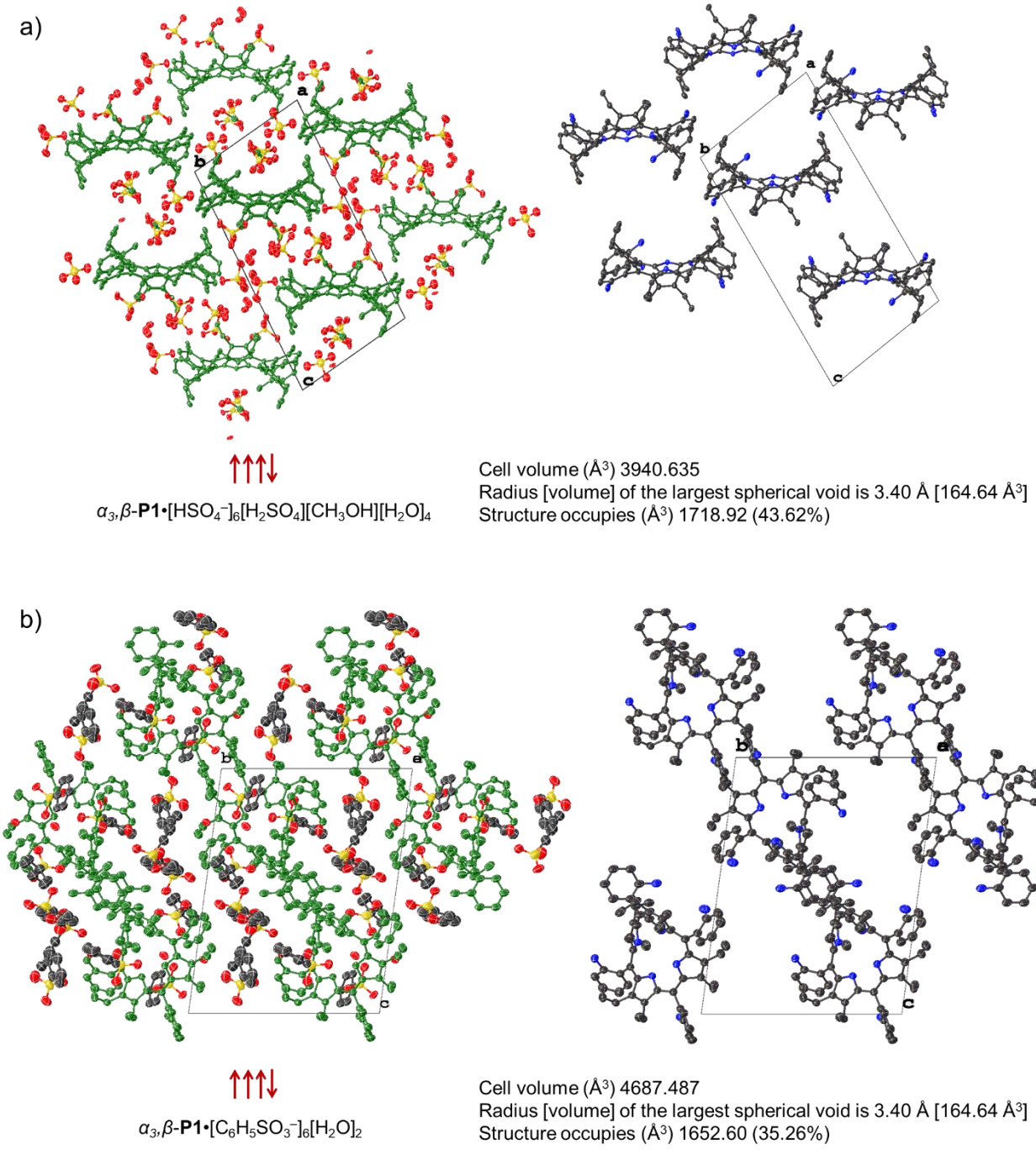

Figure S43. Crystal packing illustrations of a) *α*3,*β*-**P1**•[HSO_4^-]6[H_2SO_4][CH_3OH][H_2O]4 and b) *α*3,*β*-**P1**•[$C_6H_5SO_3^-$]6[H_2O]2. On the left, single units are highlighted in green; on the right, representation of single units without counter anions and solvents (non-essential hydrogen atoms omitted for clarity and thermal ellipsoids give 50% probability).

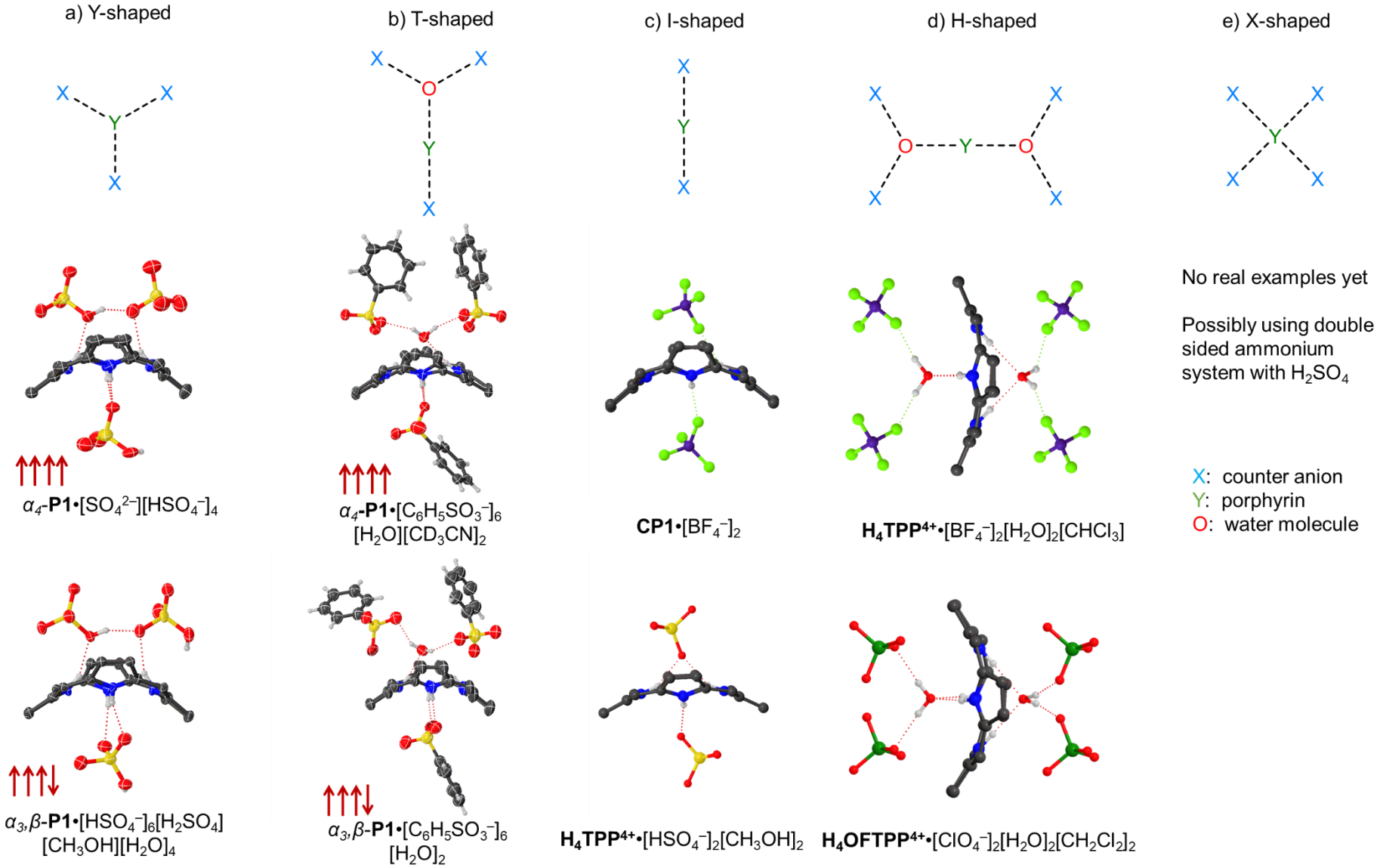

Figure S44. Core interactions observed in various protonated porphyrins showing different type complexes: a) T-shaped; b) Y-shaped ; c) I-shaped ; d) H-shaped; e) X-shaped**.** See figure S40 and S41 for more structural detail. (meso- and β-substituents and non-essential hydrogen atoms omitted for clarity and thermal ellipsoids give 50% probability).

SUPPORTING INFORMATION

Table S4. Summary of protonated porphyrins deposited in the Cambridge Crystallographic Data Centre (CCDC).

No.	Database Identifier	Deposition Number	Counter anion	Binding mode	No.	Database Identifier	Deposition Number	Counter anion	Binding mode
1	ANIHIQ	1477658	ClO_4^-	I	39	QARCAQ	1506817	CF_3COO^-	I
2	ASUNAD	238703	Cl^-	I	40	QEZKIP	159608	CF_3COO^-	I
3	BASJUA	118284	CF_3COO^-	I	41	QOSYUT	718407	Cl^-	I
4	BEJDIG	1496256	$BiCl_6^{3-}$	I	42	QURRAY	1058018	$C_6H_2(NO_2)_3O^-$	I
5	CETPEX	614470	CF_3COO^-	I	43	RALVAC	257492	CF_3COO^-	I
6	COFYAY	688606	$C_5H_4NCOO^-$	I	44	RARQEJ	1544022	Cl^-	I*
7	FARBEI	1431307	$C_6H_2(NO_2)_3O^-$	I	45	RATXUI	1498506	CF_3COO^-	I
8	FATQUP	956522	CF_3COO^-	I	46	REVROZ	1248861	ClO_4^-	I
9	FIMRAV	247692	Cl^-	I	47	RUHQAM	1252430	ClO_4^-	I
10	FOKZUC	700701	Cl^-	I	48	RUHQEQ	1252431	ClO_4^-	I
11	GOBSOF	113958	CF_3COO^-	I	49	RUHQIU	1252432	ClO_4^-	I
12	GOBYIF	113963	CF_3COO^-	I	50	SEPVIT	272182	CF_3COO^-	I
13	GUZMUJ	209626	$C_6H_2(NO_2)_3O^-$	I	51	TIQLAH	626214	Cl^-	I
14	KEVDAT	1549180	Cl^-	I	52	TIQLEL	626215	Cl^-	I
15	KIBLIQ	140336	CF_3COO^-	I	53	TIQLIP	626216	Cl^-	I
16	KIBMAJ	140337	CF_3COO^-	I	54	TPPFEC	1275452	Cl^-	I
17	KIBMEN	140338	CF_3COO^-	I	55	TPYPRC10	1275614	Cl^-	I
18	KIBPEQ	140340	CF_3COO^-	I	56	VACSIC	188053	Cl^-	I
19	KIBPEQ01	140339	CF_3COO^-	I	57	VOGZAT	670105	Cl^-	I
20	LEXSIQ	122174	HSO_4^-	I	58	WINXEW	1294090	CH_3COO^-	I
21	LEYFOK	122173	$CH_3SO_4^-$	I	59	WIXDIT	1868761	$CF_3SO_3^-$	I
22	LEYFUQ	122172	CF_3COO^-	I	60	WIXZAF	644581	BF_4^-	H
23	LEYHIG	122171	CF_3COO^-	I	61	WUKBOT	152532	ClO_4^-	H
24	LEYPEK	122177	Cl^-	I	62	XAQKOR	866745	Cl^-	I
25	LEYQAH	122178	CF_3COO^-	I	63	XARVIW	280014	CF_3COO^-	I
26	LOGMOJ	116299	$CH_3SO_3^-$	I	64	XEDFOD	866776	ClO_4^-	I
27	LOLPOR	147305	$C_8H_7O_3$	I	65	XEDFUJ	866777	ClO_4^-	I
28	MANHOZ	221910	CF_3COO^-	I	66	XEDGAQ	866778	Cl^-	I
29	MANHUF	237514	CF_3COO^-	I	67	XEDGEU	866779	Cl^-	I
30	MANJAN	238568	CF_3COO^-	I	68	XEKDEZ	1563442	CF_3COO^-	I
31	MIGNEW	654893	Cl^-	I	69	XOSYAI	1935664	HSO_4^-	Y
32	NICPEV	644176	$CHB_{11}Cl_{11}^-$	I	70	YEVJAN	1301876	ClO_4^-	I
33	NUFTEO	727607	$C_{10}H_7COO^-$	I	71	YEVKAL	122175	CF_3COO^-	I**
34	NUHKUW	1223952	Cl^-	I	72	YEVKIT	1301879	CF_3COO^-	I
35	OCAQAN	1012816	HSO_4^-	I	73	YEVKIT01	122176	CF_3COO^-	I
36	OCIQEY	825053	OH^-	I	74	YEVKOZ	1301880	CF_3COO^-	I*
37	PACXEY	793068	$C_{10}H_9FeCOO^-$	I	75	YEVKUF	1301881	CF_3COO^-	I
38	PEZXAW	1576905	Cl^-	I					

*Binary heterogeneous binding mode. In RARQEJ the secondary counter anion is 4-(1-benzylpyridin-1-ium-4-yl)benzoate; In EVKOZ the secondary counter anion is acetate.

**'cis'-protonated porphyrin

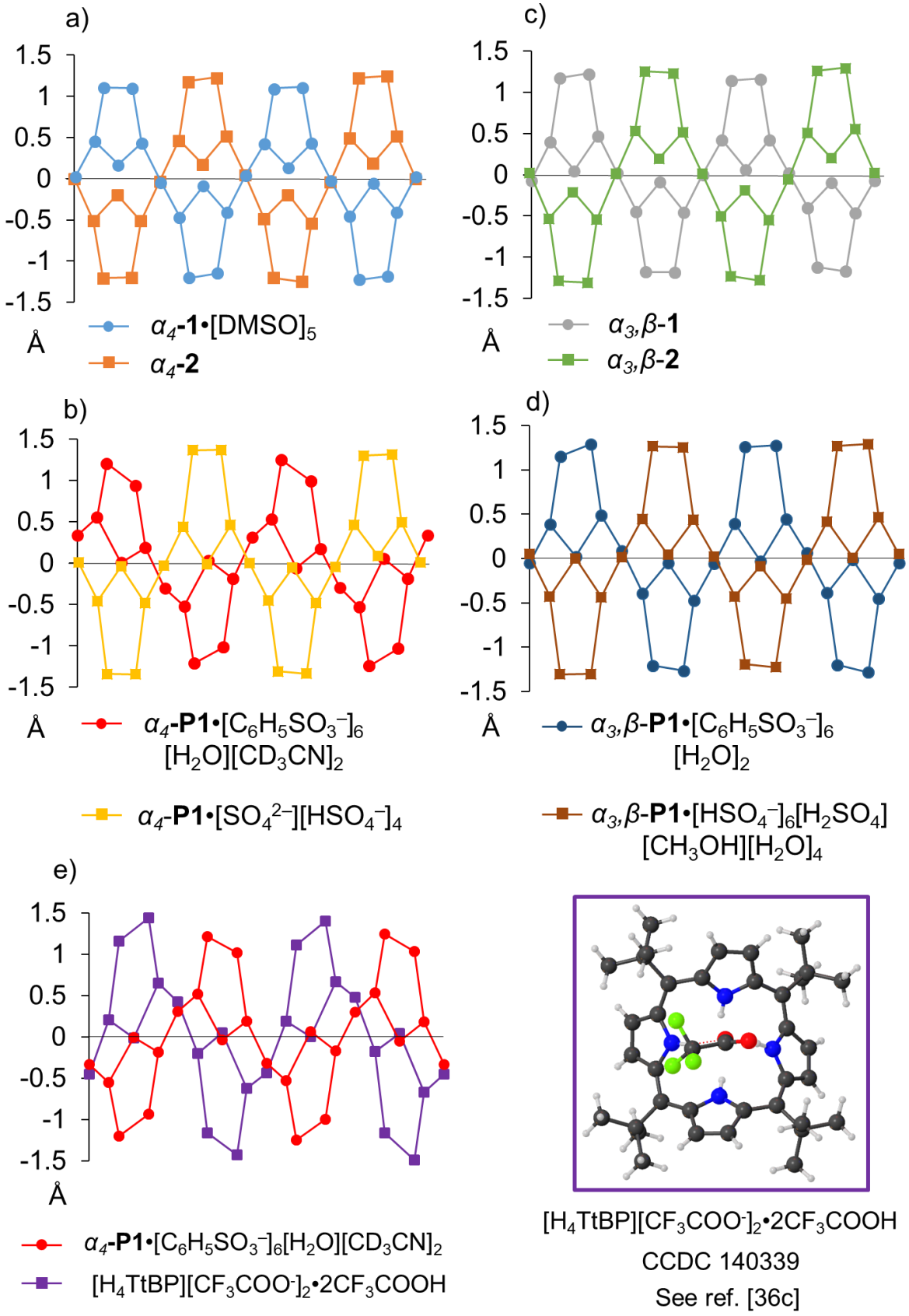

Figure S45. Linear display of the skeletal deviations: a) free base ↑↑↑↑ **1** (light blue) and Ni(II) ↑↑↑↑ **2** (orange); b) ↑↑↑↑ **P1** with H_2SO_4 (yellow) and **BSA** (red); c) free base ↑↑↑↓ **1** (grey) and Ni(II) ↑↑↑↓ **2** (green); d) ↑↑↑↓ **P1** with H_2SO_4 (brown) and **BSA** (dark blue); e) ↑↑↑↑ **P1** with **BSA** (red) and H_4TtBP with TFA.[36c]

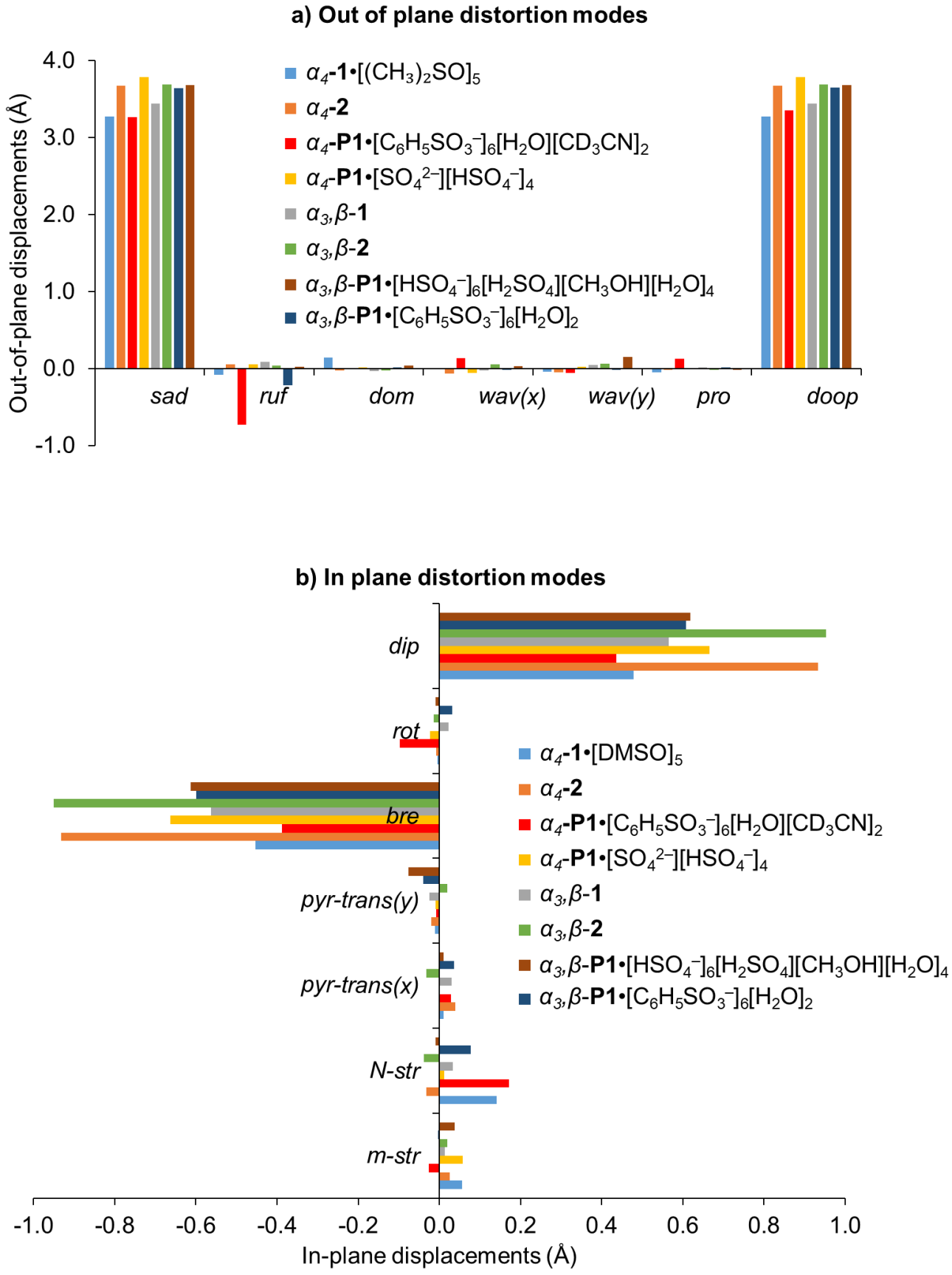

Figure S46. Illustration of the a) out-of-plane and b) in-plane normal-coordinate structural decomposition results for ↑↑↑↑ and ↑↑↑↓ atropisomers in free base **1**, Ni(II) **2** and protonated **P1** with H_2SO_4 and **BSA** forms.

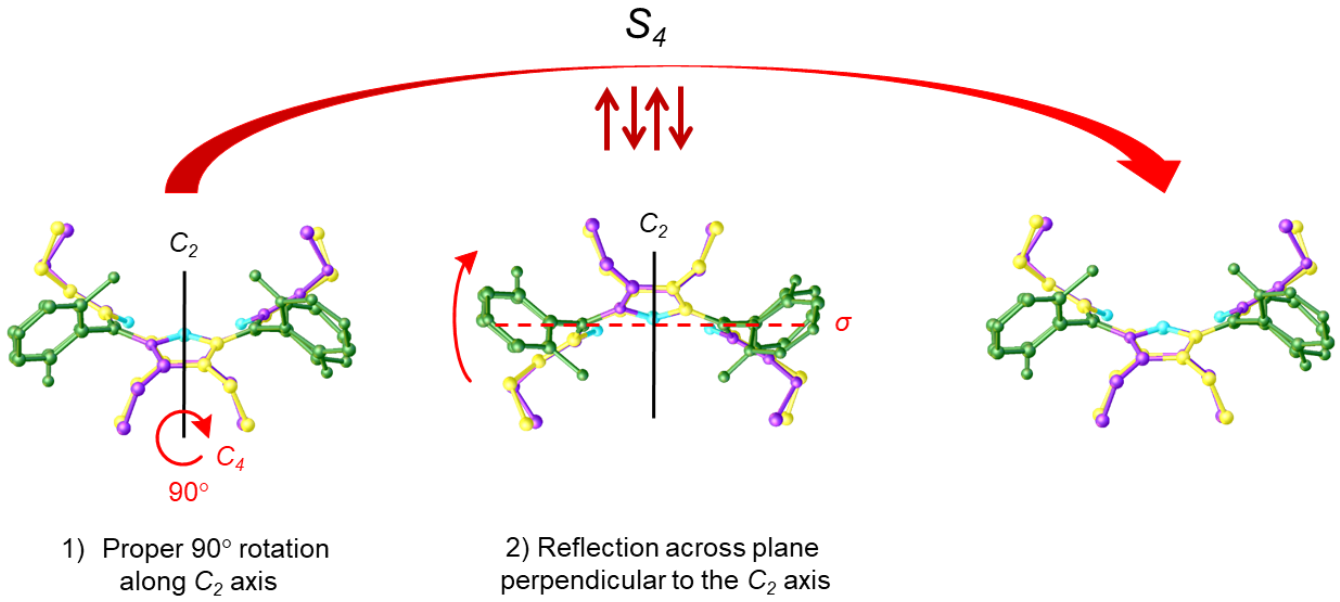

Figure S47. Improper rotation represented in the *α,β,α,β*-**P1** atropisomer. The X-ray crystal structure of *α,β,α,β*-**2** was used to visualize the symmetrical units observed from NMR analysis.

References

[S1] APEX3, Version 2016.9-0, Bruker AXS, Inc., Madison, WI, **2016**.
[S2] SADABS, Version 2016/2, Bruker AXS, Inc., Madison, WI, **2014**.
[S3] W. Jentzen, X.-Z. Song, J. A. Shelnutt, *J. Phys. Chem. B* **1997**, *101*, 1684–1699.
[S4] L. Sun and J. A. Shelnutt, NSDGUI (Version 1.3 Alpha version), Sandia National Laboratory, Albuquerque, USA., **2000–2001**.
[S5] H. Hope, *Prog. Inorg. Chem.* **2007**, *41*, 1–19.
[S6] a) O. V. Dolomanov, L. J. Bourhis, R. J. Gildea, J. A. K. Howard, H. Puschmann, *J. Appl. Cryst.* **2009**, *42*, 339–341; b) G. Sheldrick, *Acta Crystallogr.* **2015**, *A71*, 3–8.